

## Chapitre 6 : Identification d'un complexe de protéines retrouvé à l'appareil de Golgi et important pour le cycle érythrocytaire asexué chez *Plasmodium falciparum*.

---

### 6.1 Avant-propos

Le manuscrit présenté dans ce chapitre est intitulé « Identification of a Golgi apparatus protein complex important for the asexual erythrocytic cycle of the malaria parasite *Plasmodium falciparum* » a été accepté pour publication le 26 mars 2018 dans la revue « Cellular Microbiology » (**Hallée, S., Thériault, C., Gagnon, D., Kehrer, J., Frischknecht, F., Mair, G. R. & Richard, D. Cellular Microbiology e12843 (2018)**) et dont je suis la première auteure. Cette articles et présenté tel que publié. J'ai effectué l'ensemble des expériences réalisées chez *Plasmodium falciparum*, analysé les résultats et écrit le manuscrit. Catherine Thériault a effectué certaines des expériences de « pull- down » de GP2 avec GP1. Gunnar R. Mair, Jessica Kehrer et Friedrich Frischknecht ont réalisé et analysé les expériences chez *Plasmodium berghei*. Dave Richard a supervisé le projet et participé la rédaction du manuscrit. Gunnar R. Mair a participé à la révision du manuscrit.

## 6.2 Résumé

Comparativement aux autres types de cellules eucaryotes, les parasites de la malaria semblent posséder un appareil de Golgi plus rudimentaire composé d'une seule citerne dispersée en régions cis et trans. Bien que jouant un rôle central dans la voie de sécrétion du parasite, peu de protéines retrouvées dans l'appareil de Golgi ont été caractérisées chez *Plasmodium falciparum*. Nous avons précédemment identifié une nouvelle protéine résidente de l'appareil de Golgi, exerçant une fonction inconnue que nous avons nommée « Golgi Protein 1 ». Dans cet article nous montrons que cette dernière forme un complexe avec une protéine transmembranaire jusque-là non caractérisée (« Golgi Protein 2», GP2). Ce complexe de protéines de Golgi se localise au cis-Golgi tout au long du cycle érythrocytaire et potentiellement aussi lors les stades exprimés chez l'insecte vecteur anophèle. L'analyse de souches de parasites où l'expression de GP1 est conditionnellement réprimée et/ou le gène GP2 est inactivé, révèle que bien que le complexe « Golgi Protein » ne soit essentiel à aucun stade du cycle parasitaire, il semble être important pour le développement asexué lors du stade sanguin.

**Identification of a Golgi apparatus protein complex important for the asexual erythrocytic cycle of the malaria parasite *Plasmodium falciparum*.**

Stéphanie Hallée<sup>1</sup>, Catherine Theriault<sup>1</sup>, Dominic Gagnon<sup>1</sup>, Jessica Kehrer<sup>2</sup>, Friedrich Frischknecht<sup>2</sup>, Gunnar R. Mair<sup>2,3</sup> and Dave Richard<sup>1\*</sup>

<sup>1</sup> Centre de recherche en infectiologie, CHU de Québec-Université Laval Québec City, Québec, Canada, G1V 4G2 PH:1-418-525-4444 ext 47975 FAX: 1-418-654-2715

<sup>2</sup> Integrative Parasitology, Department of Infectious Diseases, University of Heidelberg Medical School, Im Neuenheimer Feld 324, 69120, Heidelberg, Germany

<sup>3</sup> Current address: Iowa State University Biomedical Sciences, 1800 Christensen Drive, 2008 Vet Med, Ames, IA 50011-1134

\*: Corresponding author and Lead Contact

E-mail: dave.richard@crchudequebec.ulaval.ca (DR)

**Keywords:** Malaria, Plasmodium, Golgi apparatus, protein complex, gene knock out

## 6.3 Abstract

Compared to other eukaryotic cell types, malaria parasites appear to possess a more rudimentary Golgi apparatus being composed of dispersed, unstacked cis and trans-cisternae. Despite playing a central role in the secretory pathway of the parasite, few Plasmodium Golgi resident proteins have been characterized. We had previously identified a new Golgi resident protein of unknown function which we had named Golgi Protein 1 and now show that it forms a complex with a previously uncharacterized transmembrane protein (Golgi Protein 2, GP2). The Golgi Protein complex localizes to the cis-Golgi throughout the erythrocytic cycle and potentially also during the mosquito stages. Analysis of parasite strains where GP1 expression is conditionally repressed and/or the GP2 gene is inactivated reveals that though the Golgi Protein complex is not essential at any stage of the parasite life cycle, it is important for optimal asexual development in the blood stages.

## 6.4 Introduction

Malaria is one of the most important infectious diseases in the world and despite all the efforts to control the disease, the World Health Organization still reported 212 million cases and 429 000 deaths in 2015 (WHO, 2016). The deadliest causative agent of malaria, *Plasmodium falciparum*, is transmitted to humans by a mosquito vector and develops within mature red blood cells (Miller et al., 2002). The development and survival of the parasite inside the erythrocyte requires the remodeling of the host cell and the formation of *de novo* merozoites during the course of a life cycle. Like most eukaryotic cell types, the malaria parasite relies on a secretory pathway to traffic newly synthesized proteins to various destinations including the secretory organelles such as the rhoptries and micronemes, the apicoplast, the digestive vacuole, or to be exported to the red blood cell cytoplasm and surface (Waller et al., 2000, Cooke et al., 2004, Kats et al., 2008, Deponte et al., 2012). Proteins possessing a signal peptide or a transmembrane domain are translated and co-translocated into the endoplasmic reticulum (ER) where their integrity is monitored by quality control mechanisms such as the endoplasmic-reticulum-associated protein degradation (ERAD) pathway. Properly folded proteins then continue their route through to the Golgi apparatus whilst misfolded proteins are translocated back to the cytosol for degradation by the proteasome (Chung et al., 2012, Deponte et al., 2012). The Golgi is a key hub of the secretory pathway, and in a typical eukaryotic cell it is composed of three functionally distinct compartments: a cis, a medial and a trans-cisterna where proteins are sorted and packaged into transport vesicles through interaction with transmembrane escorters and adaptor proteins (Becker et al., 1996, Adisa et al., 2007, Richard et al., 2009, Brandizzi et al., 2013, Krai et al., 2014). In *Plasmodium*, the Golgi appears to be more rudimentary being composed of dispersed, unstacked cis and trans-cisternae (Adisa et al., 2007, Struck et al., 2008a, Struck et al., 2008b).

Our previous work determined that the *P. falciparum* Putative Rhoptry Protein 2 (PRP2, PF3D7\_1320000) resided in the Golgi and not in the rhoptries which led us to rename it Golgi Protein 1 (GP1) (Tufet-Bayona et al., 2009, Hallee et al., 2015). We here show that GP1 interacts with a unique and previously uncharacterized transmembrane protein (PF3D7\_1123500) which we have named Golgi Protein 2 (GP2). Using a combination of conditional knockdowns and knockouts, we show that the protein complex is important but likely not essential for the in vitro asexual erythrocytic cycle. Furthermore, we show that inactivating *P. berghei* GP2 has no impact on the mosquito stages and on virulence in mice.

## 6.5 Results

### **GP1 interacts with an uncharacterised transmembrane protein**

In order to characterize the role of GP1 in *P. falciparum* blood stages, we identified interacting partners by performing an anti-HA immunoprecipitation (IP) paired with mass spectrometry (MS) analysis on the previously described GP1-RFA (regulatable fluorescent affinity) tagged line (Hallee et al., 2015). The results revealed several proteins with one candidate standing out with 42 peptides identified, an uncharacterized conserved protein PF3D7\_1123500 (hereafter named Golgi Protein 2, GP2). GP2 was the protein with the second highest number of peptides after GP1 (Table S1). GP2 is a transmembrane protein of 1336 amino acids conserved in *Plasmodium spp.* but with no significant homology outside the *Plasmodium* genus. A BLAST analysis (<https://blast.ncbi.nlm.nih.gov/Blast.cgi>) using full length GP2 failed to identify homologous proteins in related organisms like *Toxoplasma* and other apicomplexans (not shown). GP2 is predicted to possess a signal peptide and two transmembrane domains at its C-terminal end (Figure S1A).

### **GP2 potentially localises to the Golgi apparatus throughout the lifecycle of the malaria parasite**

To characterize GP2 we first endogenously tagged the protein with a triple hemagglutinin (HA) epitope by single cross-over recombination. A glucosamine-inducible glmS ribozyme was also incorporated within the 3' untranslated region to allow the conditional regulation of the protein (Figure S1B) (Prommana et al., 2013). The proper integration of the 3HA-glmS cassette at the GP2 locus was verified by Southern blot (Figure S1C) in addition to PCR genotyping (Figure S1Di). Furthermore, no wild type allele was detected in the GP2-3HA- glmS tagged line after three Blasticidin drug selection cycles (Figure S1C-Dii).

We also raised GP2 specific antibodies against a synthetic peptide comprising amino acids 259 to 272. (Figure S2A). A Western Blot performed on mixed-stage parasite protein extracts shows that the anti-GP2 serum recognizes a protein at the expected size of around 150 kDa in both *P. falciparum* 3D7 parasites and in the GP2-3HA-glmS parasite clone. Furthermore, an anti-HA Western blot revealed a single band of the same size in the tagged line only (Figure S2B). We next localized GP2 in schizont stage parasites by immunofluorescence assay (IFA) using the anti-GP2 and the anti-HA on the GP2-3HA-glmS tagged line. Both antibodies exhibited the punctate pattern typical of a Golgi-resident protein and the important overlap demonstrated that both antibodies can specifically recognize GP2 (Figure S2C)(Struck et al., 2005, Struck et al., 2008b). The extensive colocalization between GP2 and the cis-Golgi apparatus marker Endoplasmic reticulum Retention Defective 2 (ERD2) (Elmendorf et al., 1993) confirmed that GP2 resides in the Golgi throughout the blood stages

(Figure 1A). This staining pattern was conserved in the rodent malaria parasite *P. berghei*, where we tagged the endogenous locus of the orthologous gene PBANKA\_092480 with GFP. The tagged protein was also detected in gametocytes, as well as all mosquito stage parasites including the ookinete, midgut oocysts, and sporozoites providing evidence for the constitutive expression of GP2 throughout the life cycle of the parasite (Figure 1B and Figure S3). In addition, the staining pattern of PbGP2 in the mosquito stages resembled what was previously described with PbGP1 which suggests that they might perhaps also form a complex in this phase of the life cycle (Tufet-Bayona et al., 2009).

To confirm the interaction between GP1 and GP2, we performed an anti-HA IP on GP1-RFA parasites and probed with the anti-GP2 antibody. The IP was also done on GP2-3HA-glmS and a 3D7 line as positive and negative controls, respectively. A specific 150 kDa band was seen in both tagged lines but not in the wild-type control, confirming that GP2 interacts with GP1 in *P. falciparum*. The absence of ERD2 in the IP eluate further suggests that GP2 does not bind in a non-specific way to all Golgi proteins (Figure 1C). An IFA on GP1-RFA late stage parasites using anti-HA and anti-GP2 antibodies showed strong co-localization between both signals which would be expected if GP1 and GP2 form a complex (Figure 1D).

### **Identification of a GP1 interacting domain in GP2.**

To characterize the GP1-GP2 interaction in more detail, in vitro pull-down assays were performed. We first decided to express two large regions situated between the SP and the first transmembrane domain of GP2 (fragments A and B) (Figure 2A). The proper expression and purification of GP2 fragments coupled to the GST tag was validated by SDS-Page and Coomassie staining (Figure S4). Incubation of the GP2 fragments with GP1-RFA parasite lysate showed that only the A construct corresponding to the region comprising amino acids 239 to 571 was able to interact with GP1 (Figure 2Bi). The A region was then further subdivided in two parts (C and D) and only the D fragment was able to pull down GP1 (Figure 2Bii). Analysis of the secondary structure of this region (corresponding to amino acids 438 to 560) using the Jpred4 platform (Drozdetskiy et al., 2015) predicted four  $\alpha$ -helices followed by one  $\beta$ -sheet (Figure 2A). Based on this information we systematically narrowed down the interacting domain to the last two  $\alpha$ -helix and the  $\beta$ -sheet of GP2 (AA503 to 555) (Figure 2Biii). GP1 possesses a signal peptide (SP) and no TM so it is likely found inside the Golgi (Banfield, 2011). The presence of the GP1 binding domain of GP2 between the SP and the first TM suggests that it is also inside the organelle and not facing outside, in the cytoplasm.

### **Identification of potential GP1 and GP2 interacting partners**

To identify interactors of GP2, we performed an IP-MS analysis using the GP2-3HA-glmS line together with 3D7 parasites as negative control. Table S2 lists all the potential interacting partners with an enrichment of at least 2 fold above the control. As with the GP1-RFA IP, the proteins with the highest number of peptides were GP2 and GP1 (67 peptides and 23 peptides identified, respectively). To try to identify other proteins putatively interacting with the GP1- GP2 complex, we looked at proteins with a least a 2-fold enrichment in both IPs (Table S3). Interestingly, two proteins associated with the ERAD pathway were recovered: Ubiquitin- activating enzyme E1 (PF3D7\_1225800, UBA1), and Protein disulfide isomerase (PF3D7\_0827900). We also found two mitochondrial proteins, one tRNA ligase, one RNA binding protein, a protein involved in nuclear export and the enzyme 6-phosphofructokinase. Based on their known functions and subcellular localisations, these proteins are unlikely to be true interactors of the GP1-GP2 complex. Finally, the merozoite surface protein MSP1 was also identified as a potential interactor. Since MSP1 transits through the secretory pathway on its way to the parasite plasma membrane, it could indeed encounter the GP protein complex. This might suggest that the GP complex could act as an escort to MSP1 however the lack of an obvious defect in MSP1 trafficking in parasite lines where the expression of GP1 is decreased and of GP2 is completely abolished makes it unlikely (see below).

#### **Knockdown of GP1 affects in vitro *P. falciparum* asexual stage parasite growth.**

The inability to inactivate *P. berghei* GP1 previously suggested that it was essential in the blood stages (Tufet-Bayona et al., 2009). To determine whether this was the case in *P. falciparum*, we attempted to knock out the GP1 gene using the newly developed selection- linked integration for targeted gene disruption strategy (SLI-TGD). This method provides greatly increased efficiency in the selection of parasites with genomic integrations (Birnbaum et al., 2017). Despite numerous attempts, we were unable to delete GP1 (data not shown).

We had previously unsuccessfully tried to conditionally regulate the expression of GP1 by using the DHFR destabilization domain (Muralidharan et al., 2011, Halle et al., 2015) so we decided to switch to the glmS ribozyme system and generated a marker-free GP1-3HA-glmS tagged line by using the CRISPR-Cas9 technology (Figure S5A) (Ghorbal et al., 2014, Theriault et al., 2017). Proper integration of the 3HA-glmS cassette at the 3' end of the GP1 gene was verified by Southern Blot and PCR before and after parasite cloning (Figure S5B- C). Anti-HA Western blot on GP1-3HA-glmS protein extracts showed a band of around 80 kDa which is smaller than the expected size of 150 kDa (Figure S5D). This was also seen with the GP1-RFA strain which led us to speculate that GP1 was potentially processed. Incubation of the GP1-3HA-glmS line with glucosamine (GlcN) revealed a specific dose dependent decrease in GP1-3HA expression (Figure 3A and B). Of interest, the

expression of GP2 was not affected by the down regulation of GP1 (Figure 3A). We next looked at the effect of the GP1 KD on parasite growth and saw a mild reduction in parasitaemia of around 30% after three cycles (Figure 3C). The absence of an effect of GlcN on the GP1-RFA line control demonstrates that the decreased growth observed is not due to a toxic effect of the compound (Figure 3D).

### **Knock out of GP2 affects GP1 levels and negatively impacts in vitro asexual stage parasite growth.**

To explore the role of GP2 in the asexual erythrocytic stages we incubated the GP2-3HA- glmS line described above (Figure S1) with increasing concentrations of GlcN resulting in a dose dependent decrease in the intensity of the anti-GP2 signal compared to the anti-GAP50 loading control (Figure 4Ai). Densitometric analysis of the signal intensity showed an almost complete knockdown of the GP2-3HA protein at 2.5 mM GlcN (Figure 4Aii). We next performed growth curve analysis in the presence or absence of 2.5 mM GlcN and the parasitaemia was monitored every 24 h for 120 h (three life cycles) by FACS (Figure 4B). Despite the almost complete absence of GP2-HA, no effect was seen on parasite growth when compared to a wild type control suggesting that either GP2 is not essential for asexual life cycle progression, or that minimal protein levels are sufficient to perform its function. To try to confirm this, we attempted to inactivate the GP2 gene using SLI-TGD (Figure S6A). In contrast to GP1, we succeeded in knocking out the GP2 gene which was confirmed by PCR detection of the proper integration of the pSLI-TGD-GP2 vector at the GP2 locus and the absence of the WT allele (Figure S6B). A Western blot using the anti-GP2 antibody showed that the GP2 protein was no longer present in the GP2KO line (Figure S6C). Analysis of the growth of the GP2KO strain showed a decrease of around 25% in the parasitemia compared to the 3D7 control (Figure S6D) demonstrating that GP2 is not essential but still plays an important role in in vitro asexual growth.

To test the effect of a simultaneous decrease in both GP1 and GP2 protein expression we tried to knock out GP2 in the GP1-3HA-glmS tagged line using SLI-TGD (Figure S7A). Proper integration of the vector and disappearance of the WT allele were detected by PCR (Figure S7B) whilst the absence of detectable GP2 by Western blot using the anti-GP2 antibody confirmed that we had successfully inactivated the GP2 gene in the GP1-3HA-glmS line (Figure S7C). Intriguingly, inactivating GP2 led to a decrease of around 75% in the amount of GP1-3HA to even lower levels than in the GP1-3HA-glmS knocked down line (i.e. incubated with 2.5 mM GlcN, around 50% decrease in GP1-3HA levels) (Figure 5A and B). Knocking down GP1-3HA in the GP2KO/GP1-3HA-glmS line led to a further reduction in its expression (around 90% reduction compared to GP13HA-glmS levels) (Figure 5A and B). Some reduction in the level of GP1-3HA was also

observable by IFA though it did not look as extensive as on the Western blots (Figure 5Ci vs iii and iv). In addition, the usual punctate fluorescence pattern of GP1-3HA was slightly disrupted in the GP2 KO with some small portion of it looking like it remained trapped close to the nucleus, potentially in the ER (Figure 5Ci vs iii). By increasing the exposure time to capture more HA signal, we saw that the residual punctate pattern still colocalised with ERD2 suggesting that in absence of GP2, a significant amount of GP1-3HA was still trafficked to the Golgi (Figure 5D). Interestingly, this sort of phenotype is reminiscent, though certainly not as striking, of what was seen with the low molecular weight rhoptry protein complex where RAP1 escorts RAP2 to the rhoptries and in absence of the former, the latter stays trapped in the ER. Though a decrease in the levels of RAP2 in the RAP1KO strain is seen by Western, it is not that striking when looking at IFA images (Baldi et al., 2000). Globally, these results suggest that GP2 might potentially be required for the optimal localization of GP1 to the Golgi apparatus.

To determine the effect of the absence of GP2 combined with the reduced expression of GP1-3HA on parasite survival, we followed the growth of the parasites over three cycles by FACS. As seen in the GP2KO in the 3D7 WT line, inactivating GP2 in the GP1-3HA-glmS line led to a 25% reduction in growth (Figure 5E: dark blue curve, KO-GP2-GP1-glmS-0mM vs dark green curve, GP1-3HA-glmS 0mM), around what we obtained with the GP1 KD line (Figure 5E: light green curve, GP1-3HA-glmS-2.5mM vs dark green curve, GP1-3HA-glmS 0mM). Decreasing the expression of GP1-3HA in the GP2 KO line led to an additive effect with a 44% reduction in parasitaemia (Figure 5B: light blue curve, KOGP2-GP1-glmS- 2.5mM vs dark green curve, GP1-3HA-glmS 0mM). Globally, these data suggest that the GP1-GP2 protein complex is important but perhaps not essential for the in vitro erythrocytic cycle of *P. falciparum*.

In order to provide insight into the function of the GP1-GP2 complex, we further characterized the GP1-3HAKD/GP2KO parasite line. We first followed the evolution in stage distribution of the parasites over three growth cycles and did not see any changes (Figure S8A). Next, analysis of the invasiveness of purified merozoites showed no deficiency (Figure S8B). Finally, we investigated by IFA whether the localisation of different organellar markers was affected in the KD/KO line. Only some minor effects were noticeable for the microneme markers AMA1 and EBA175, the inner membrane complex protein GAP45 and the merozoite surface protein MSP1 (Figure S9). Globally, the lack of any obvious specific defect might suggest that general parasite fitness is affected.

### **Inactivation of *P. berghei* GP2 reveals that it is dispensable throughout the life cycle.**

To investigate the role of GP2 in the virulence to mice and on the mosquito stage, we inactivated the GP2 gene in *P. berghei* (Figure 6A). The rodent malaria gene deletion mutant infected the mosquito vector similar to WT numbers. Infectious sporozoites isolated from salivary glands showed no apparent defects in motility (Figure 6B and C) and produced patent mouse infections between days 4 and 5 (Figure 6D), comparable to the WT strain. This demonstrates that PbGP2 is not required at any step of the rodent malaria life cycle.

In conclusion, we have identified a *Plasmodium*-specific Golgi protein complex important but likely not essential for the in vitro asexual erythrocytic cycle of the human parasite *P. falciparum*. Moreover, we show that *P. berghei* GP2 is not required for the mosquito stages nor for virulence in a mouse model of infection.

## 6.6 Discussion

Here we report on the identification and characterization of a new protein complex within the malaria parasite Golgi apparatus that is important for the *P. falciparum* asexual blood stages. GP1 was initially reported as a putative rhoptry protein in *P. berghei* (Tufet-Bayona et al., 2009) but we subsequently showed that the *P. falciparum* homologue was in fact residing in the Golgi and not the rhoptries. We have now determined that GP1 forms a complex with a unique *Plasmodium* uncharacterized transmembrane protein that we named Golgi Protein 2 (GP2). Recently, GP2 was identified in a BioID screen for parasitophorous vacuole proteins (Khosh-Naucke et al., 2017) but the data presented here using tagged *P. falciparum* and *P. berghei* lines as well as GP2 specific antibodies clearly show that it is present in the Golgi.

The potential interaction of proteins involved in the ERAD pathway with the GP complex is interesting as GP1 and GP2 are mostly found in the Golgi and not in the ER where ERAD takes place. However, this in itself does not rule out the possibility that they play a role in this pathway as some cis-Golgi proteins are known to be involved in ER processes; for example, ERD2 is critical for retrograde vesicular trafficking from the Golgi to the ER (Elmendorf et al., 1993, Kulzer et al., 2009). The *P. falciparum* ERAD system has been proposed to be essential and recombinant *P. falciparum* ERAD components have been shown to mediate ubiquitylation in vitro (Chung et al., 2012). It is tempting to speculate that the GP complex is also participating in this ER quality control process. Of interest, *Plasmodium* parasites have duplicated several members of the ERAD pathway and repurposed them to act as a translocation machinery in the apicoplast (apERAD) (Kalanon et al., 2009, Spork et al., 2009, Agrawal et al., 2013), an endosymbiont organelle of algal origin (McFadden et al., 1996, Kohler et al., 1997). However, none of the apERAD proteins interacted with the GP complex during immunoprecipitation.

Recent work has shown that GP1 is partially similar to the autophagy related protein 2 (Atg2) of *Saccharomyces cerevisiae* (Kitamura et al., 2012). Autophagy is a process whereby cellular material such as misfolded proteins are degraded inside the lysosome (Yang et al., 2009). In *P. falciparum*, various roles have been suggested for autophagy proteins (Atg) such as trafficking to the food vacuole, organelle expulsion and protein secretion (Hain et al., 2013), and apicoplast inheritance (Bansal et al., 2017). Despite the recent interest in *Plasmodium* autophagy, several *Plasmodium* Atg homologues remain to be identified. In yeast, Atg2 establishes a complex with Atg9 (a 6 transmembrane domains protein) and Atg18 (a phosphatidylinositol triphosphate binding protein) and is involved in the formation of pre- autophagosomal structure during the preliminary step of

autophagy (Tanida, 2011, Hain et al., 2013). A homologue of Atg18 has been identified in *P. falciparum* (PF3D7\_1012900) and it has recently been shown to be critical for the inheritance of the apicoplast (Wang et al., 2016, Bansal et al., 2017). Of note, PfAtg18 was not found in our list of GP1 interacting proteins. No *P. falciparum* homologue for Atg9 has been found as of now (Hain et al., 2013) but the related apicomplexan *Toxoplasma gondii* does possess a homologue of Atg9 that localizes to the Golgi (Nguyen et al., 2017). Since GP2 contains only two predicted transmembrane domains, it is unlikely that it would serve a similar function as Atg9.

The potential association of ERAD components to GP1-GP2 and the homology of GP1 to yeast Atg2 could suggest a role of the protein complex in the stress response. In *T. gondii*, no growth defect was seen when a TgAtg9 KO strain was grown under nutrient rich conditions (Nguyen et al., 2017) which fits with the fact that autophagy is not essential under normal *in vitro* growth conditions for several other eukaryotic cell types (Tsukada et al., 1993). To try to look for a potential involvement of the GP1/GP2 complex in ERAD, we looked at the level of protein ubiquitinylation by Western blot and also tested the sensitivity of the KD/KO parasites to the ER stressing agent DTT. In both cases, the results were highly variable between experiments (results not shown) which precluded us to reach a conclusion. Perhaps exposing our GP1KD/GP2KO parasite line to other stressing agents like artemisinin would reveal increased sensitivity (Navale et al., 2014). In any case, more work will be necessary to investigate the potential link between the GP1-GP2 complex and autophagy and/or the ERAD pathway.

We initially hypothesized that GP2 was anchoring GP1 to the inside of the Golgi membrane and that this was required for its function. The fact that we were not able to knockout GP1 but succeeded with GP2 is intriguing since our data shows that in absence of GP2, GP1 levels are reduced and a significant portion of the protein is potentially mislocalised to the ER. This suggests that only a small amount of GP1 is required for proper asexual *in vitro* growth. This is further supported by the fact that GP1KD/GP2KO parasites are still viable though with a close to 50% reduction in parasitaemia. The use of a conditional knock out strategy like the recently described DiCre system (Collins et al., 2013) will be required to determine whether GP1 is truly essential or not and to gain a better understanding of its function.

## 6.7 Materials and Methods

Study approved by the Canadian Blood Services (CBS) research ethics board, project number 2015.001 and by the CHU de Québec IRB, project number 2015–2230, B14-12-2230, SIRUL 104595. Written consent was obtained by the CBS for all study participants. All experiments were performed in accordance with relevant guidelines and regulations.

### Parasite culture

*P. falciparum* 3D7 were maintained in human O+ erythrocytes at a hematocrit of 4% with 0.5% (w/v) Albumax<sup>TM</sup> (Invitrogen) in RPMI medium (Life Tech). *P. falciparum* 3D7 parasite were originally obtained from David Walliker at Edinburgh University. Cultures were synchronized by incubation with 0.3 M alanine for 10 min (Braun-Breton et al., 1988).

### Cloning and transfection

All primers used for cloning are listed in Table S1 and all plasmids were sequenced and analyzed before transfection. The GP2 recombinant fragments were PCR amplified from *P. falciparum* gDNA and cloned in pGEX-6P3 using BamHI-XhoI restriction enzymes in frame with a GST tag.

To tag the 3' end of the GP1 gene with the 3HA-glmS cassette, a CRISPR-Cas9 strategy was utilised (Zhang et al., 2014). First, the pL7-GP1-3HA-glmS vector was made using the vector pL6-3HA-glmS-BSD (Therault et al., 2017). The FL5 fragment corresponding to a 1 kb of the 3' end of the coding region was cloned XhoI-XmaI in frame with the 3HA-glmS cassette. Then the FL3 fragment corresponding to the 5' extremity of the 3'UTR region of GP1 was cloned SacII-SpeI. Finally, the gRNA was made by annealing primers fwgRNA-GP1 and revgRNA-GP1 and the resulting gRNA was cloned by InFusion (Clontech) (in pL6-FL5- GP1-3HA-glmS-FL3-BSD digested BtgZI. *P. falciparum* 3D7 parasite were transfected with 60 µg of each purified plasmid; pL7-GP1-3HA-glmS and pUF-CAS9-yDHOD (Promega) (Volz et al., 2016). Transfectants were selected with 2.5 mg/ml Blasticidin (Sigma-Aldrich) and 30 nM N-(3-chloro-4-methylphenyl)-5-methyl-2-(trifluoromethyl) [1,2,4] triazolo[1,5-a] pyrimidin-7-amine (ChemBridge) (diluted in RPMI) for 6 days then all drugs were removed.

Parasite were then cloned by limiting dilution without drugs and cloned cultures were genotyped by PCR (see primer list in Supplementary Table S2) and Southern Blot according to standard procedures.

To generate the GP2-3HA-glmS line, a fragment of 1049 bp of the 3' end of GP2 gene was amplified without the stop codon on 3D7 *P. falciparum* genomic DNA. The fragment was then cloned NotI-

AvrII upstream the 3HA-glmS cassette in p3HA-glmS-BSD, where the hDHFR resistance gene had been replaced by the Blasticidin deaminase (BSD) resistance gene (Prommana et al., 2013). *P. falciparum* 3D7 parasites were transfected with 100 µg of purified plasmid DNA (Promega). Integrated parasites were selected using 2.5 mg/ml Blasticidin (Sigma-Aldrich) and cloned as previously described (Gilberger et al., 2003).

To attempt the knockout (KO) of GP1 and GP2, we used the recently described selection- linked integration for targeted gene disruption (SLI-TGD) strategy (Birnbaum et al., 2017). We generated the pSLI-TGD-GP1 vector by amplifying, on 3D7 *P. falciparum* gDNA, a fragment of 497pb at the 5' extremity of the GP1 gene and cloned it into NotI-MluI restriction sites of the pSLI-TGD vector. The pSLI-TGD-GP2 construct was obtained by cloning a fragment from nucleotides 55-540 of the GP2 gene into pSLI-TGD using NotI- MluI. *P. falciparum* 3D7 (for GP1 KO and GP2 KO) or GP1-3HA-glmS (for GP2 KO only) parasites were transfected with 100 µg of purified plasmid and parasites were first selected with 10 nM WR99210 (Jacobus Pharmaceuticals) until reappearance and then put on 0,25mg/ml G418 (Sigma-Aldrich) in triplicate for 3 weeks. Proper integration of the vectors was detected by PCR (see primer list in Supplementary Table 1).

### **Southern Blot**

Integration of GP1-3HA-glmS and GP2-3HA-glmS were confirmed by Southern blot according to standard procedure. Briefly, gDNA was extracted from parasites using the Blood genomic DNA extraction kit (Sigma). For each parasite line, 10 µg of gDNA was digested with PstI-NheI (GP2) or HindIII-EcoRI (GP1). Digested DNA fragments were separated on 0.7% (w/v) agarose gel then transferred on Hybond N+ membrane (GE) and hybridized with radiolabeled probe.

### **Western blot and Immunoprecipitation**

To test the GP2 specific antibody and the 3HA-glmS tagged lines, schizonts of 3D7 *P. falciparum*, GP2-3HA-glmS or GP1-3HA-glmS parasites were extracted using 0.15% saponin and pellets were resuspended in SDS protein sample buffer. Proteins were then separated on 7% (w/v) SDS-PAGE gel under reducing conditions and transferred to a PVDF membrane (Milipore). The membrane was blocked in 4% (w/v) milk in TBS-T. Antibodies used were mouse monoclonal anti-HA 1:2000 (Cedarlane, clone HA.C5); mouse monoclonal anti-Aldolase 1:1000 (Immunology Consultants Inc., MB720); rabbit polyclonal GP2 1:2000 (GL Biochem Shanghai); rabbit polyclonal GAP50 1:2000 (Jones et al., 2006). Appropriate HRP-coupled secondary antibodies were used and immunoblots were developed using ECL (Bio-Rad).

To directly verify the GP1 and GP2 interaction, immunoprecipitation followed by Western blot analysis was performed. Schizont parasites of GP1-RFA, GP2-3HA-glmS and *P. falciparum* 3D7 were isolated with 0.15% saponin and proteins extracted with 1% T-NET buffer (1% TX-100, 50 mM Tris pH 7.4, 150 mM NaCl, 5 mM EDTA) with cOmplete protein inhibitor (Roche). Parasite lysates were then incubated with anti-HA affinity matrix (Roche) and washed with PBS. Washed beads were directly resuspended in sample buffer and analyzed by Western blot using the rabbit polyclonal GP2 1:2000 (GL Biochem Shanghai) and a rabbit polyclonal anti-ERD2 1:2000 (Elmendorf et al., 1993). The specific antibodies were raised against the GP2 peptide DHHDEKGDGHPLEH (amino acids 259- 272).

To test the protein regulation with the glmS system, tightly synchronous young rings of GP1- 3HA-glmS and GP2-3HA-glmS parasites were treated with increasing concentrations of glucosamine (GlcN), from 0 mM up to 5 mM. Parasites were harvested in the same cycle at the schizont stage, then saponin-lysed and resuspended in SDS protein sample buffer. Membranes were probed with a mouse monoclonal anti-HA 1:2000 (Cedarlane, clone HA.C5), rabbit polyclonal GP2 1:2000 (GL Biochem Shanghai) and mouse monoclonal anti- Aldolase 1:1000 (Immunology Consultants Inc., MB720) as loading control. The intensity of the signal was quantified and compared with the loading control using the Fiji software and a dose response curve was fit using Graph Prism v6.

The effect of the knockout of GP2 on GP1 expression was investigated by incubating GP1- 3HA-glmS and GP2-KO in GP1-3HA-glmS parasites lines with or without 2.5 mM GlcN for one cycle. Schizonts were harvested by 0.15% saponin treatment and parasite pellets directly resuspended in sample buffer. Protein expression was analysed by Western blot using anti- HA 1:2000 (Cedarlane, clone HA.C5) and mouse monoclonal anti-Aldolase 1:1000 (Immunology Consultants Inc., MB720) as loading control.

## **Microscopy**

Fluorescence microscopy acquisition was performed as previously described (Hallee et al., 2015) using a GE Applied Precision Deltavision Elite microscope with 100x 1.4NA objective and with a sCMOS camera and deconvolved with the SoftWorx software. In immunofluorescence assays, parasites were fixed on slide using 4% paraformaldehyde (ProSciTech), permeabilized with 0.1% Triton-X100 then blocked in 3% bovine serum albumin (BSA fraction V, EMD). The slides were then probed with a combination of antibodies: mouse anti-HA 1:1000 (Cedarlane, clone HA.C5); rabbit polyclonal GP2 1:2000 (GL Biochem Shanghai); rabbit anti-ERD2 1:1000 (MRA-72) (Elmendorf et al., 1993); rabbit anti-Bip 1:500 (Absalon and Dvorin, unpublished), rabbit anti-

PfEMP1 ATS 1:200 (Maier et al., 2007). Primary antibodies were probed with Alexa Fluo 594 anti-rabbit IgG or anti-mouse IgG (Molecular Probes) and Alexa Fluor 488 anti-Rabbit IgG or anti-mouse IgG (Cell Signaling). Slides were mounted with 4',6-Diamidino-2-phenylindole dihydrochloride (DAPI, Invitrogen, 100ng/ul) in VectaShield (Vector Labs).

For the GP1 knockdown and GP2 knockout analysis, tightly synchronized parasites were treated at the young ring stage with or without 2.5 mM GlcN and parasites were imaged at the schizont stage of the same cycle. A panel of antibodies were utilized in combination with the mouse anti-HA 1:1000 (Cedarlane, clone HA.C5) or rabbit polyclonal anti-HA (Abm, 1:1000): mouse anti-RAP1 (1:3000); mouse anti-RON4 (1:2000) (Richard et al., 2010); rabbit anti-AMA1 (1:2000) (Healer et al., 2005); mouse anti-EBA175 (MRA711A, 1:500) (Sim et al., 2011)(50); rabbit anti-GAP45 (1:2000) (Jones et al., 2006)(51); rabbit anti-MSP1 (1:1000) (Wilson et al., 2011); rabbit anti-SERA5 (1:1000) (Stallmach et al., 2015); rabbit anti-ERD2 (1:1000). For mitochondrion analysis, Mitotracker Red (Molecular Probes, 10 nM) was used in live imaging combined with DAPI.

### **Mass spectrometry analysis**

Briefly  $7 \times 10^9$  schizonts from the GP1-RFA or GP2-3HA-glmS and *P. falciparum* 3D7 (control) lines were saponin extracted. Parasites were lysed in 1% Triton X-100 buffer with cOmplete protein inhibitor cocktails (Roche) then incubated with anti-HA affinity matrix (Roche), spun and then washed with PBS. Bound proteins were sent directly for LC-MS/MS analysis. Proteins digestion and mass spectrometry experiments were performed by the Proteomics platform of the CHU de Quebec Research Center, Quebec, Canada. Briefly, beads were washed 3 times with 50 mM ammonium bicarbonate buffer and kept at  $-20^{\circ}\text{C}$  until trypsin digestion. Proteins on beads were suspended in 25  $\mu\text{l}$  50 mM ammonium bicarbonate and Trypsin (1  $\mu\text{g}$ ) was added and sample was incubated overnight at  $37^{\circ}\text{C}$ . Trypsin reaction was stopped by acidification with 3% acetonitrile-1% TFA-0.5% acetic acid. Beads were removed and the peptides were purified on stage tip (C18) and vacuum dried before MS injection. Samples were solubilized into 15  $\mu\text{l}$  of 0.1% formic acid and 5  $\mu\text{l}$  were analyzed by MS using a TripleTOF 5600 mass spectrometer fitted with a nanospray III ion source (ABSciex, Concord, ON) and coupled to an Agilent 1200 HPLC. 2  $\mu\text{l}$  samples were injected by the Agilent 1200 autosampler onto a 0.075 mm (internal diameter) self-packed PicoFrit column (New Objective) packed with an isopropanol slurry of 5  $\mu\text{m}$  Jupiter C18 (Phenomenex) stationary phase using a pressure vessel set at 700 p.s.i. The length of the column was 15 cm. Samples were run using a 65min gradient from 5-35% solvent B (solvent A 0.1% formic acid in water; solvent B: 0.1% formic acid in acetonitrile) at a flow rate of 300 nl/min. Data was acquired using an ion spray voltage of 2.4kV, curtain gaz of 30 PSI, nebulizer gaz of 8 PSI and an interface heater temperature of  $125^{\circ}\text{C}$ . An

information- dependent acquisition (IDA) method was set up with the MS survey range set between 400 amu and 1250 amu (250msec) followed by dependent MS/MS scans with a mass range set between 100 and 1800 amu (50m sec) of the 20 most intense ions in the high sensitivity mode with 2+ to 5+ charge state. Dynamic exclusion was set for a period of 3 sec and a tolerance of 100 ppm.

#### Database Searching

MGF peak list files were created using Protein Pilot version 4.5 software (ABSciex) utilizing the Paragon and Progroup algorithms (Shilov). MGF sample files were then analyzed using Mascot (Matrix Science, London, UK; version 2.5.1). They were set up to search the PlasmoDB database (5542 entries) assuming the digestion enzyme trypsin. Mascot was searched with a fragment ion mass tolerance of 0.10 Da and a parent ion tolerance of 0.10 Da. Oxidation of methionine, deamidation of asparagine and glutamine were specified as variable modifications and carbamidomethylation (C) as a fixed modification. Two missed cleavages were allowed.

#### Criteria for protein identification

Scaffold (version 4.8.3), Proteome Software Inc., Portland, OR) was used to validate MS/MS based peptide and protein identifications. Protein and peptide FDR rate was set to 1% based on decoy database searching with a minimum of 1 peptides per protein. Protein probabilities were assigned by the Protein Prophet algorithm (Nesvizhskii et al., 2003). Proteins that contained similar peptides and could not be differentiated based on MS/MS analysis alone were grouped to satisfy the principles of parsimony.

#### **Recombinant protein expression and Pull-down assay**

The GP2 protein was divided into 9 fragments based on the secondary structure of the protein (Jpred4; Jnet version: 2.3.1; [http://www.compbio.dundee.ac.uk/jpred4/index\\_up.html](http://www.compbio.dundee.ac.uk/jpred4/index_up.html)) (Drozdetskiy et al., 2015)(19). The GP2 fragments were fused to a GST tag and expressed as recombinant proteins in *E. coli* BL21 and were purified using glutathione-agarose beads (Sigma). Recombinant protein expression was confirmed by SDS-PAGE and Coomassie blue staining. For the Pull-down assay, parasites of GP1-RFA were resuspended in 1% T-NET with cOmplete protease inhibitor (Roche) followed by mild sonication on ice. After an extraction period of 45 min on ice, insoluble material was separated by centrifugation. The soluble fraction was incubated with the purified proteins coupled to glutathione-agarose beads then washed with wash buffer (20 mM Tris pH 7.4, 150 mM NaCl). Washed beads were directly resuspended in sample buffer and analyzed by Western blot using the mouse anti-HA 1:2000 (Cedarlane, clone HA.C5) and mouse monoclonal anti-Aldolase 1:1000 (Immunology Consultants Inc., MB720) as loading control.

### **Growth assay and conditional knockdown analysis**

For the growth assay, parasites were treated with or without 2.5 mM GlcN (Sigma). Parasitaemia was set at 0.5% with 4% hematocrit in a 12 well plate and parasite growth was monitored at 24, 72 and 120 hours post induction. Each condition was done in triplicate. Briefly, at each time point a sample was taken and stained with SYBRGold (Invitrogen- Molecular Probe) then fixed with 1% paraformaldehyde. Samples were then analyzed by fluorescence activated cell sorting (FACS) using a BD FACSCanto and FACSDiva acquisition software and post-analyzed using FlowJo software. Uninfected red blood cells were used to determine the threshold for FITC signal. For each sample, 100000 total events were recorded. The percentage of survival was obtained by normalizing to untreated parasites in the same experiment, which were taken as 100% survival. Data were analyzed for statistical significance for each time point using two-way ANOVA followed by a Tukey multiple comparison test. Experiments were performed in biological triplicate.

To detect a defect in schizont rupture or a merozoite invasion, the number of schizonts remaining and the number of rings produced at 52 h post induction were determined by FACS. The percentage of schizonts remaining and the percentage of rings produced were normalized compared to the untreated condition. Data were analyzed for statistical significance using Graph Prism V6 and the Kruskal-Wallis non-parametric with Dunn's multiple comparisons test. Experiments were performed in biological triplicate.

### ***Plasmodium berghei* GP2 tagging and gene deletion**

Animal experiments performed at the University of Heidelberg were approved by the German Authorities (Regierungspräsidium Karlsruhe, Germany). For GFP tagging of the endogenous gp2 allele (PBANK\_0924800) a 1040 bp PCR product (primers g3179, g3180) was cloned in frame with GFP using EcoRI and BamHI resulting in plasmid pLIS0383. *P. berghei* schizonts were transfected with PacI-linearised plasmid as described and mutants selected with pyrimethamine (Janse et al., 2006). For gp2 deletion two homologous flanking regions [primers g3177, g3180 (KpnI, HindIII); primers g3179, g3180 (EcoRI, BamHI) were cloned either side of the hdhfr selection marker resulting in plasmid pLIS0385. The construct was linearised with KpnI and BamHI and transfected as described; mutants were selected with pyrimethamine and clonal lines established by limiting dilution (Janse et al., 2006). All primer sequences including those used for PCR genotyping are shown in Table S1.

### **Oocyst and sporozoite production; transmission experiments.**

Mosquito oocyst and sporozoite numbers were determined through standard infections, allowing *Anopheles stephensi* mosquitoes to blood-feed for 20 minutes on anaesthetised *P. berghei*-infected NMRI mice 3 days post transfer of 20million bloodstage parasites (gp2::gfp or  $\Delta$ gp2). Isolated midguts on days 11-12 were stained with 0,1% mercurochrome and oocyst numbers were then determined, sporozoite were isolated between days 17-25. For mosquito to mouse transmission 10k wild type or  $\Delta$ gp2 sporozoites were injected intra-venously into C57Bl6 mice and parasite numbers were subsequently determined by counting Giemsa- stained blood smears until day 9.

### ***P. berghei* live microscopy and *in vitro* gliding motility**

Live images of gp2::gfp parasites were taken on a Nikon Spinning Disc (100× objective) fluorescence microscope. Sporozoite gliding motility assays were recorded on a Zeiss 200M Axiovert widefield microscope (25x objective) for 3-5min using a frame rate of 3s (Kehrer et al., 2016, Santos et al., 2017). Image processing was performed with ImageJ. Speed was determined using the manual tracking plugin.

## 6.8 Acknowledgments

We would like to thank the following people for providing reagents: Julian Rayner, Alan Cowman and Jacobus Pharmaceuticals. The following reagents were obtained through MR4 as part of the BEI Resources, NIAID, NIH: Polyclonal Anti-Plasmodium falciparum PfERD2 (antiserum, Rabbit), MRA-1. Human erythrocytes were kindly provided by the Canadian Blood Services. This study was funded through a Canadian National Sciences and Engineering Research Council Discovery Grant (Grant number 418192-2012) to DR and a European Research Council grant (StG 281719) to FF. FF is a member of the excellence cluster CellNetworks at Heidelberg University.

## 6.9 References

1. Adisa, A., Frankland, S., Rug, M., Jackson, K., Maier, A.G., Walsh, P., et al. (2007). Re- assessing the locations of components of the classical vesicle-mediated trafficking machinery in transfected *Plasmodium falciparum*. *International Journal for Parasitology* **37**, 1127-1141.
2. Agrawal, S., Chung, D.-W.D., Pons, N., van Dooren, G.G., Prudhomme, J., Brooks, C.F., et al. (2013). An Apicoplast Localized Ubiquitylation System Is Required for the Import of Nuclear-encoded Plastid Proteins. *PLoS pathogens* **9**, e1003426.
3. Baldi, D.L., Andrews, K.T., Waller, R.F., Roos, D.S., Howard, R.F., Crabb, B.S. and Cowman, A.F. (2000). RAP1 controls rhoptry targeting of RAP2 in the malaria parasite *Plasmodium falciparum*. *The EMBO journal* **19**, 2435-2443.
4. Banfield, D.K. (2011). Mechanisms of protein retention in the Golgi. *Cold Spring Harb Perspect Biol* **3**, a005264.
5. Bansal, P., Tripathi, A., Thakur, V., Mohammed, A. and Sharma, P. (2017). Autophagy- Related Protein ATG18 Regulates Apicoplast Biogenesis in Apicomplexan Parasites. *MBio* **8**.
6. Becker, B. and Melkonian, M. (1996). The secretory pathway of protists: spatial and functional organization and evolution. *Microbiol Rev* **60**, 697-721.
7. Birnbaum, J., Flemming, S., Reichard, N., Soares, A.B., Mesen-Ramirez, P., Jonscher, E., et al. (2017). A genetic system to study *Plasmodium falciparum* protein function. *Nat Methods* **14**, 450-456.
8. Brandizzi, F. and Barlowe, C. (2013). Organization of the ER-Golgi interface for membrane traffic control. *Nat Rev Mol Cell Biol* **14**, 382-392.
9. Braun-Breton, C., Rosenberry, T.L. and da Silva, L.P. (1988). Induction of the proteolytic activity of a membrane protein in *Plasmodium falciparum* by phosphatidyl inositol- specific phospholipase C. *Nature* **332**, 457-459.
10. Chung, D.-W.D., Pons, N., Prudhomme, J., Rodrigues, E.M. and Le Roch, K.G. (2012). Characterization of the Ubiquitylating Components of the Human Malaria Parasite's Protein Degradation Pathway. *PloS one* **7**, e43477.
11. Collins, C.R., Das, S., Wong, E.H., Andenmatten, N., Stallmach, R., Hackett, F., et al. (2013). Robust inducible Cre recombinase activity in the human malaria parasite *Plasmodium falciparum* enables efficient gene deletion within a single asexual erythrocytic growth cycle. *Molecular microbiology*.
12. Cooke, B.M., Lingelbach, K., Bannister, L.H. and Tilley, L. (2004). Protein trafficking in *Plasmodium falciparum*-infected red blood cells. *Trends Parasitol* **20**, 581-589.
13. Deponte, M., Hoppe, H.C., Lee, M.C.S., Maier, A.G., Richard, D., Rug, M., et al. (2012). Wherever I may roam: protein and membrane trafficking in *P. falciparum*-infected red blood cells. *Molecular and biochemical parasitology* **186**, 95-116.
14. Drozdetskiy, A., Cole, C., Procter, J. and Barton, G.J. (2015). JPred4: a protein secondary structure prediction server. *Nucleic Acids Res* **43**, W389-394.
15. Elmendorf, H.G. and Haldar, K. (1993). Identification and localization of ERD2 in the malaria parasite *Plasmodium falciparum*: separation from sites of sphingomyelin synthesis and implications for organization of the Golgi. *The EMBO journal* **12**, 4763- 4773.
16. Ghorbal, M., Gorman, M., Macpherson, C.R., Martins, R.M., Scherf, A. and Lopez-Rubio, J.- J. (2014). Genome editing in the human malaria parasite *Plasmodium falciparum* using the CRISPR-Cas9 system. *Nature biotechnology*, 1-5.
17. Gilberger, T.-W., Thompson, J.K., Reed, M.B., Good, R.T. and Cowman, A.F. (2003). The cytoplasmic domain of the *Plasmodium falciparum* ligand EBA-175 is essential for invasion but not protein trafficking. *The Journal of cell biology* **162**, 317-327.
18. Hain, A.U.P. and Bosch, J. (2013) Autophagy in Plasmodium, a multifunctional pathway?
19. Hallee, S. and Richard, D. (2015). Evidence that the Malaria Parasite *Plasmodium falciparum* Putative Rhoptry Protein 2 Localizes to the Golgi Apparatus throughout the Erythrocytic Cycle. *PLoS One* **10**, e0138626.
20. Healer, J., Triglia, T., Hodder, A.N., Gemmill, A.W. and Cowman, A.F. (2005). Functional analysis of *Plasmodium falciparum* apical membrane antigen 1 utilizing interspecies domains. *Infection and Immunity* **73**, 2444-2451.
21. Janse, C.J., Franke-Fayard, B., Mair, G.R., Ramesar, J., Thiel, C., Engelmann, S., et al. (2006). High efficiency transfection of *Plasmodium berghei* facilitates novel selection procedures. *Molecular and biochemical parasitology* **145**, 60-70.

22. Jones, M.L., Kitson, E.L. and Rayner, J.C. (2006). *Plasmodium falciparum* erythrocyte invasion: a conserved myosin associated complex. *Mol Biochem Parasitol* **147**, 74-84.
23. Kalanon, M., Tonkin, C.J. and McFadden, G.I. (2009). Characterization of two putative protein translocation components in the apicoplast of *Plasmodium falciparum*. *Eukaryot Cell* **8**, 1146-1154.
24. Kats, L.M., Cooke, B.M., Coppel, R.L. and Black, C.G. (2008). Protein trafficking to apical organelles of malaria parasites - building an invasion machine. *Traffic* **9**, 176-186.
25. Kehrer, J., Singer, M., Lemgruber, L., Silva, P.A., Frischknecht, F. and Mair, G.R. (2016). A Putative Small Solute Transporter Is Responsible for the Secretion of G377 and TRAP-Containing Secretory Vesicles during *Plasmodium* Gamete Egress and Sporozoite Motility. *PLoS Pathog* **12**, e1005734.
26. Khosh-Naucke, M., Becker, J., Mesen-Ramirez, P., Kiani, P., Birnbaum, J., Frohlike, U., et al. (2017). Identification of novel parasitophorous vacuole proteins in *P. falciparum* parasites using BioID. *Int J Med Microbiol*.
27. Kitamura, K., Kishi-Itakura, C., Tsuboi, T., Sato, S., Kita, K., Ohta, N. and Mizushima, N. (2012). Autophagy-related Atg8 localizes to the apicoplast of the human malaria parasite *Plasmodium falciparum*. *PLoS One* **7**, e42977.
28. Kohler, S., Delwiche, C.F., Denny, P.W., Tilney, L.G., Webster, P., Wilson, R.J., et al. (1997). A plastid of probable green algal origin in Apicomplexan parasites. *Science* **275**, 1485-1489.
29. Krai, P., Dalal, S. and Klemba, M. (2014). Evidence for a Golgi-to-Endosome Protein Sorting Pathway in *Plasmodium falciparum*. *PLoS one* **9**, e89771.
30. Kulzer, S., Gehde, N. and Przyborski, J.M. (2009). Return to sender: use of *Plasmodium* ER retrieval sequences to study protein transport in the infected erythrocyte and predict putative ER protein families. *Parasitol Res* **104**, 1535-1541.
31. Maier, A.G., Rug, M., O'Neill, M.T., Beeson, J.G., Marti, M., Reeder, J. and Cowman, A.F. (2007). Skeleton-binding protein 1 functions at the parasitophorous vacuole membrane to traffic PfEMP1 to the *Plasmodium falciparum*-infected erythrocyte surface. *Blood* **109**, 1289-1297.
32. McFadden, G.I., Reith, M.E., Munholland, J. and Lang-Unnasch, N. (1996). Plastid in human parasites. *Nature* **381**, 482.
33. Miller, L.H., Baruch, D.I., Marsh, K. and Doumbo, O.K. (2002). The pathogenic basis of malaria. *Nature* **415**, 673-679.
34. Muralidharan, V., Oksman, A., Iwamoto, M., Wandless, T.J. and Goldberg, D.E. (2011). Asparagine repeat function in a *Plasmodium falciparum* protein assessed via a regulatable fluorescent affinity tag. *PNAS* **108**, 4411-4416.
35. Navale, R., Atul, Allanki, A.D. and Sijwali, P.S. (2014). Characterization of the autophagy marker protein Atg8 reveals atypical features of autophagy in *Plasmodium falciparum*. *PLoS One* **9**, e113220.
36. Nesvizhskii, A.I., Keller, A., Kolker, E. and Aebersold, R. (2003). A statistical model for identifying proteins by tandem mass spectrometry. *Anal Chem* **75**, 4646-4658.
37. Nguyen, H.M., El Hajj, H., El Hajj, R., Tawil, N., Berry, L., Lebrun, M., et al. (2017). *Toxoplasma gondii* autophagy-related protein ATG9 is crucial for the survival of parasites in their host. *Cell Microbiol* **19**.
38. Prommana, P., Uthairipibull, C., Wongsombat, C., Kamchonwongpaisan, S., Yuthavong, Y., Knuepfer, E., et al. (2013). Inducible Knockdown of *Plasmodium* Gene Expression Using the glmS Ribozyme. *PLoS one* **8**, e73783.
39. Richard, D., Kats, L.M., Langer, C., Black, C.G., Mitri, K., Boddey, J.A., et al. (2009). Identification of rhoptry trafficking determinants and evidence for a novel sorting mechanism in the malaria parasite *Plasmodium falciparum*. *PLoS pathogens* **5**, e1000328.
40. Richard, D., MacRaild, C.A., Riglar, D.T., Chan, J.-A., Foley, M., Baum, J., et al. (2010). Interaction between *Plasmodium falciparum* apical membrane antigen 1 and the rhoptry neck protein complex defines a key step in the erythrocyte invasion process of malaria parasites. *The Journal of biological chemistry* **285**, 14815-14822.
41. Santos, J.M., Egarter, S., Zuzarte-Luis, V., Kumar, H., Moreau, C.A., Kehrer, J., et al. (2017). Malaria parasite LIMP protein regulates sporozoite gliding motility and infectivity in mosquito and mammalian hosts. *Elife* **6**.
42. Sim, B.K., Narum, D.L., Chattopadhyay, R., Ahumada, A., Haynes, J.D., Fuhrmann, S.R., et al. (2011). Delineation of stage specific expression of *Plasmodium falciparum* EBA- 175 by biologically functional region II monoclonal antibodies. *PLoS One* **6**, e18393.
43. Spork, S., Hiss, J.A., Mandel, K., Sommer, M., Kooij, T.W., Chu, T., et al. (2009). An unusual ERAD-like complex is targeted to the apicoplast of *Plasmodium falciparum*. *Eukaryot Cell* **8**, 1134-1145.
44. Stallmach, R., Kavishwar, M., Withers-Martinez, C., Hackett, F., Collins, C.R., Howell, S.A., et al. (2015). *Plasmodium falciparum* SERA5 plays a non-enzymatic role in the malarial asexual blood-stage lifecycle. *Mol Microbiol* **96**, 368-387.

45. Struck, N.S., de Souza Dias, S., Langer, C., Marti, M., Pearce, J.A., Cowman, A.F. and Gilberger, T.W. (2005). Re-defining the Golgi complex in *Plasmodium falciparum* using the novel Golgi marker PfGRASP. *Journal of cell science* **118**, 5603-5613.
46. Struck, N.S., Herrmann, S., Langer, C., Krueger, A., Foth, B.J., Engelberg, K., et al. (2008a). *Plasmodium falciparum* possesses two GRASP proteins that are differentially targeted to the Golgi complex via a higher- and lower-eukaryote-like mechanism. *Journal of cell science* **121**, 2123-2129.
47. Struck, N.S., Herrmann, S., Schmuck-Barkmann, I., de Souza Dias, S., Haase, S., Cabrera, A.L., et al. (2008b). Spatial dissection of the cis- and trans-Golgi compartments in the malaria parasite *Plasmodium falciparum*. *Molecular microbiology* **67**, 1320-1330.
48. Tanida, I. (2011). Autophagosome formation and molecular mechanism of autophagy. *Antioxid Redox Signal* **14**, 2201-2214.
49. Theriault, C. and Richard, D. (2017). Characterization of a putative *Plasmodium falciparum* SAC1 phosphoinositide-phosphatase homologue potentially required for survival during the asexual erythrocytic stages. *Sci Rep* **7**, 12710.
50. Tsukada, M. and Ohsumi, Y. (1993). Isolation and characterization of autophagy-defective mutants of *Saccharomyces cerevisiae*. *FEBS Lett* **333**, 169-174.
51. Tufet-Bayona, M., Janse, C.J., Khan, S.M., Waters, A.P., Sinden, R.E. and Franke-Fayard, B. (2009). Localisation and timing of expression of putative *Plasmodium berghei* rhoptry proteins in merozoites and sporozoites. *Molecular and biochemical parasitology* **166**, 22-31.
52. Volz, J.C., Yap, A., Sisquella, X., Thompson, J.K., Lim, N.T., Whitehead, L.W., et al. (2016). Essential Role of the PfRh5/PfRipr/CyRPA Complex during *Plasmodium falciparum* Invasion of Erythrocytes. *Cell Host Microbe* **20**, 60-71.
53. Waller, R.F., Reed, M.B., Cowman, A.F. and Mcfadden, G.I. (2000). Protein trafficking to the plastid of *Plasmodium falciparum* is via the secretory pathway. *The EMBO journal* **19**, 1794-1802.
54. Wang, Z., Cabrera, M., Yang, J., Yuan, L., Gupta, B., Liang, X., et al. (2016). Genome-wide association analysis identifies genetic loci associated with resistance to multiple antimalarials in *Plasmodium falciparum* from China-Myanmar border. *Sci Rep* **6**, 33891.
55. WHO (2016). World Malaria Report. Wilson, D.W., Fowkes, F.J.I., Gilson, P.R., Elliott, S.R., Tavul, L., Michon, P., et al. (2011). Quantifying the Importance of MSP1-19 as a Target of Growth-Inhibitory and Protective Antibodies against *Plasmodium falciparum* in Humans. *PloS one* **6**, e27705.
56. Yang, Z. and Klionsky, D.J. (2009). An overview of the molecular mechanism of autophagy. *Curr Top Microbiol Immunol* **335**, 1-32.
57. Zhang, C., Xiao, B., Jiang, Y., Zhao, Y., Li, Z., Gao, H., et al. (2014). Efficient Editing of Malaria Parasite Genome Using the CRISPR/Cas9 System. *mBio* **5**, e01414-01414- e01414-01414.

## 6.10 Figures

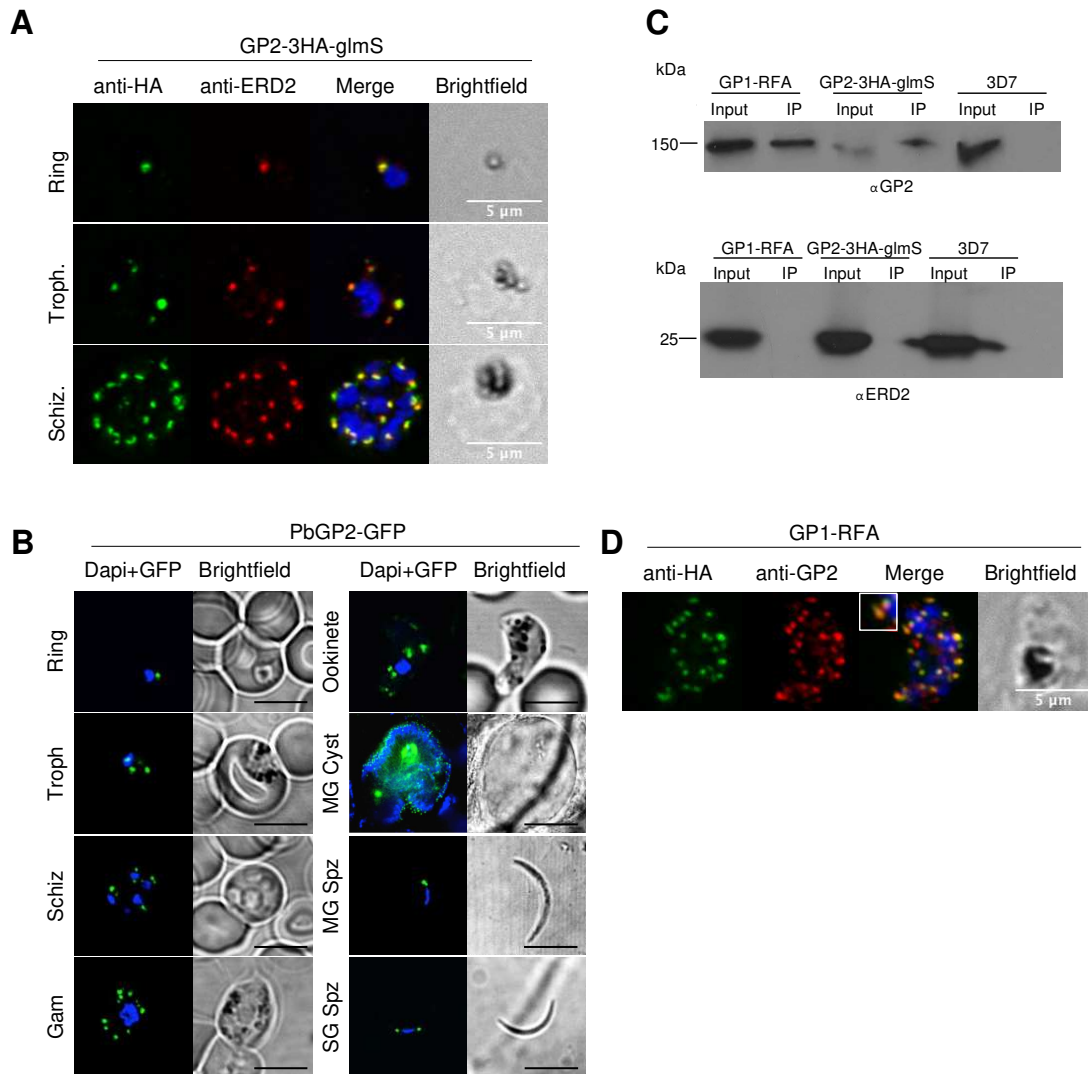


**Figure 1: The GP1-GP2 complex is localized in the Golgi apparatus throughout the asexual erythrocytic cycle and potentially the mosquito stages.** (A) GP2 colocalizes with the cis-Golgi marker ERD2 in all blood stages. (B) PbGP2 is expressed in blood and mosquito stages. Troph.: trophozoite. Schiz.: schizont. Gam: Gametocyte. MG: Midgut. SG: Salivary gland. Spz: Sporozoite. (C) Immunoprecipitation using anti-HA beads on GP1-RFA and GP2-3HA-glmS tagged lines results in the pull down of GP2 as detected using the specific anti-GP2 antibody. IP: immunoprecipitated material (D) IFA performed on GP1- RFA schizont stage parasites shows colocalization between GP1 (anti-HA, green) and GP2 (anti-GP2, red). Scale bars represent 5  $\mu$ m.

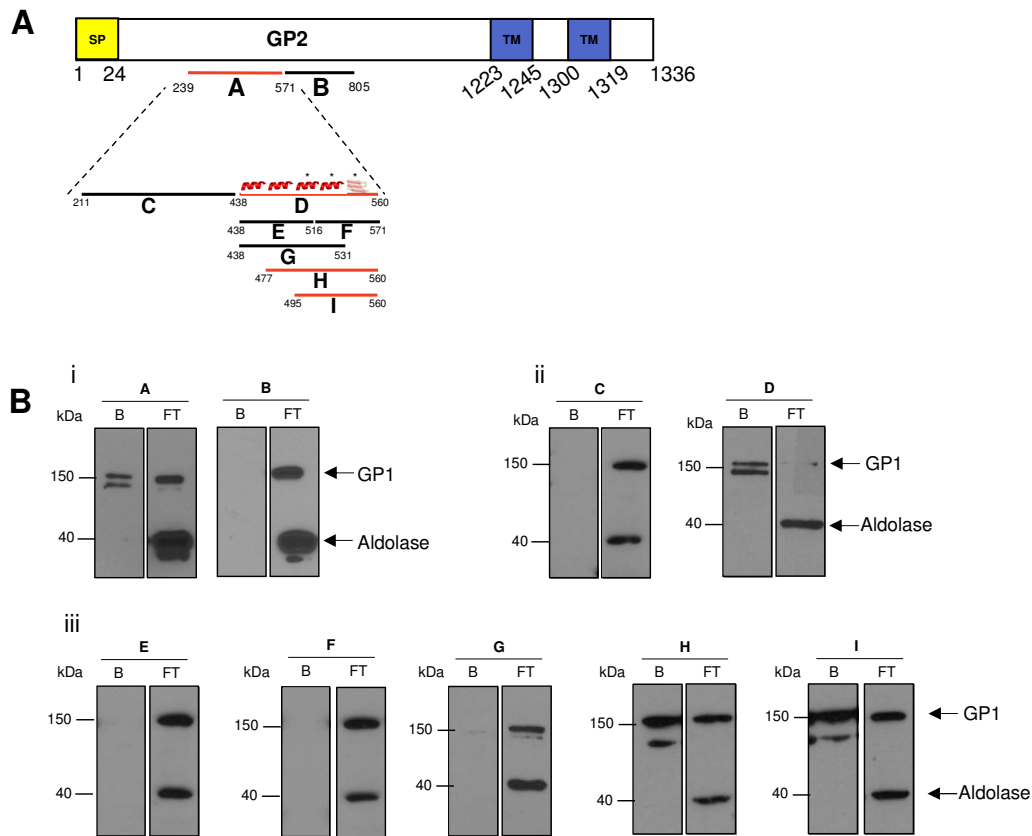


**Figure 2: GP1 interacts with GP2 in in vitro pull-down assay.** (A) Schematic of the GP2 protein showing the different regions produced as recombinant proteins. Secondary structure of the peptide is represented above peptide D (helix and sheet). Amino acid positions are indicated below each fragment. SP, signal peptide; TM, transmembrane domain; red bar indicates positive interaction with GP1; \* represents predicted secondary structures for the binding of GP1. (B) In vitro pull-down experiment shows that fragments A, D, H and I of GP2 are able to successfully pull down GP1 from GP1-RFA parasite lysate. The interaction was detected by Western blot using anti-HA (to detect GP1-RFA, 150kDa) and anti-Aldolase (40kDa) was used as loading control. Beads attached proteins and flow through (control) were loaded. B, proteins bound to beads; FT, flow through.

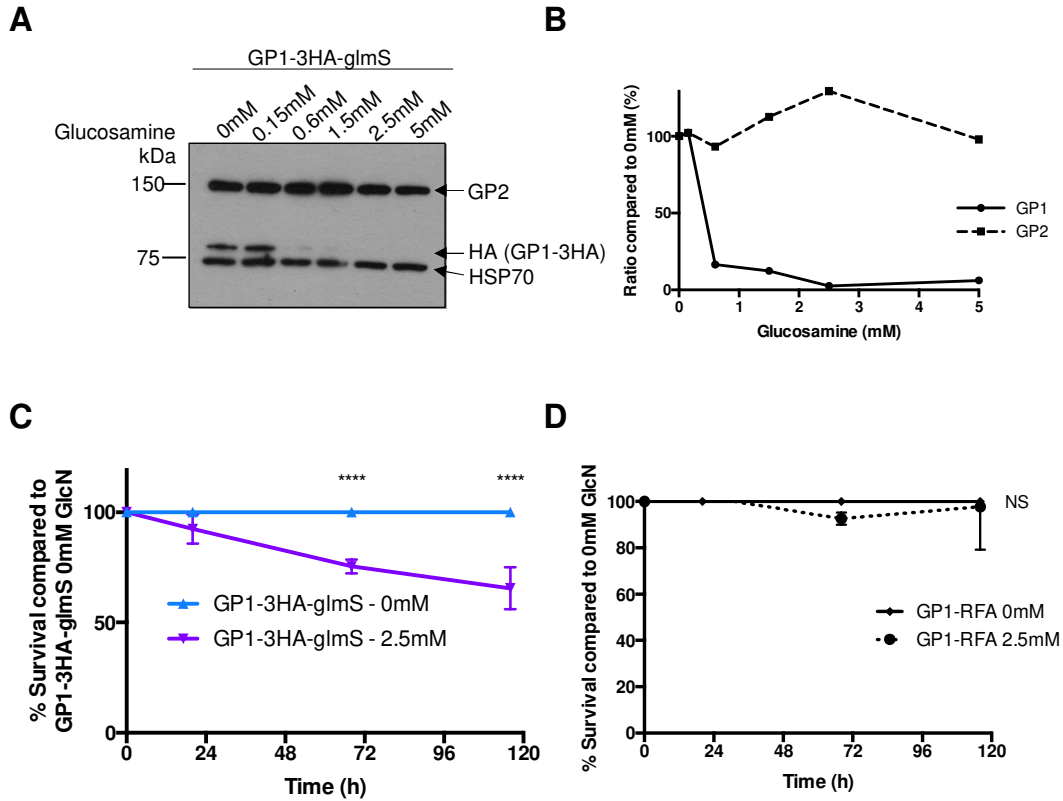


**Figure 3: Knockdown of GP1 has a slight effect on asexual erythrocytic cycle proliferation.** (A) GP1-3HA-glmS expression is regulated in a dose dependent manner when treated with increasing concentrations of glucosamine (GlcN). The expression of GP2 is not affected by the down regulation of GP1 expression in GP1-3HA-glmS. The anti-HSP70 is used as loading control. (B) Densitometry shows the ratio of anti-HA intensity compared to the loading control (anti-HSP70) for each GlcN concentrations. (C) Knocking down the expression of GP1-3HA with 2.5 mM GlcN results in an around 35% decrease in growth compared to the 0mM control over 3 cycles (116h). (D) Incubation of the GP1-RFA line with GlcN shows no effect on growth. N=3. NS=Non significant. P-values: \*\*\*\*<0.01. Multiple T test with Holm-Sidak method (alpha=5%).

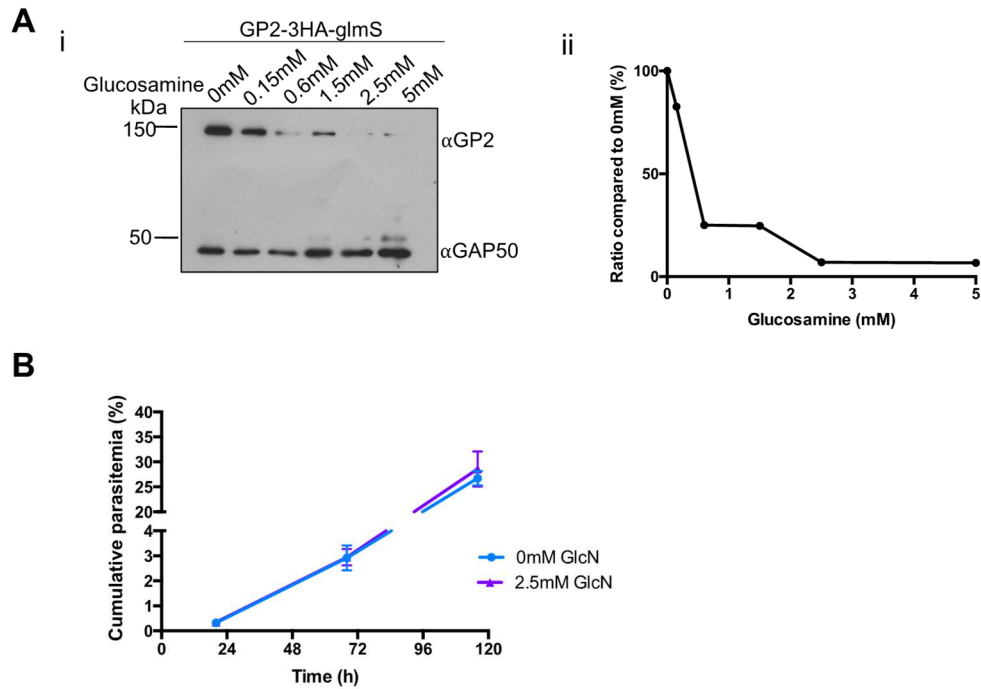


**Figure 4: Knockdown of GP2 has no effect on asexual blood stage growth.** (A) (i) Western blot using anti-GP2 shows a dose dependant regulation of GP2-3HA-glmS expression by the glmS system with increasing concentration of glucosamine. The anti- GAP50 is used as loading control. (ii) Quantification of the signal intensity shows a reduction of almost 100% of the protein expression after a treatment with 2.5 mM of glucosamine. (B) The down-regulation of GP2-3HA-glmS with 2.5 mM GlcN has no effect on parasite survival. The growth curves show no difference between the untreated and the treated parasite and this over a period of 3 cycles (116h). GlcN: Glucosamine.

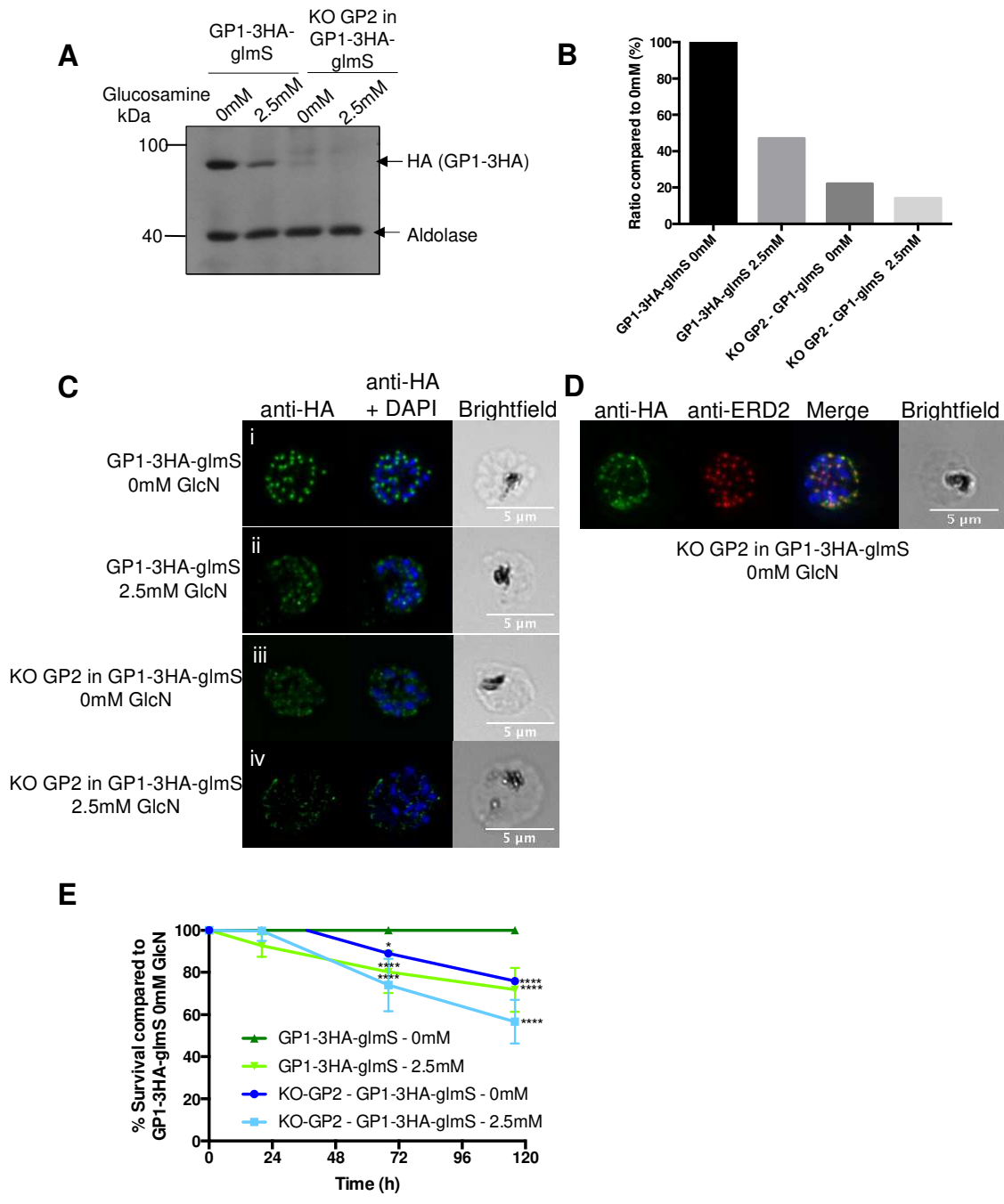


**Figure 5: Knocking down GP1 and knocking out GP2 in the same parasite line results in reduced asexual parasite survival.** (A) Knocking out GP2 reduces GP1 levels detectable by Western blot. The absence of GP2 combined with the knockdown of GP1 results in the almost complete abolition of GP1 expression compared to the knockdown in the glmS tagged line only. The anti-Aldolase is used as loading control (B) Quantification of the signal intensity shows that the KO GP2 has a decrease of around 75% of the GP1-3HA levels. Results from one experiment representative of

at least 3 biological replicates are shown. (C) IFA showing the reduction of the GP1 signal after knockdown induction (ii) compared to the untreated parasites (i) in the GP1-3HA-glmS line. (iii) Knocking out GP2 causes the mislocalisation of a portion of GP1-3HA. (iv) Knocking out GP2 and knocking down GP1 leads to an almost complete loss of the GP1 signal by IFA. Scale bar represent 5  $\mu$ m. (D) IFA showing that the residual punctate pattern of GP1-3HA in the KOGP2 line still overlaps with ERD2. Note that the green channel was overexposed to capture more HA signal and allow the colocalisation analysis. (E) Growth curve analysis reveals that knocking down GP1 and knocking out GP2 results in an additive detrimental effect on parasite survival compared to the knockout of GP2 alone or the knockdown of GP1 alone. Abrogation of the expression of these two protein results in a decrease of more than 40% of the parasitemia after three cycles. N=4 biological replicates. \*\*\*\*= $p < 0.0001$ ; \*= $p < 0.05$ ; NS=not significant. Two-way ANOVA followed by a Tukey multiple comparison test was used.

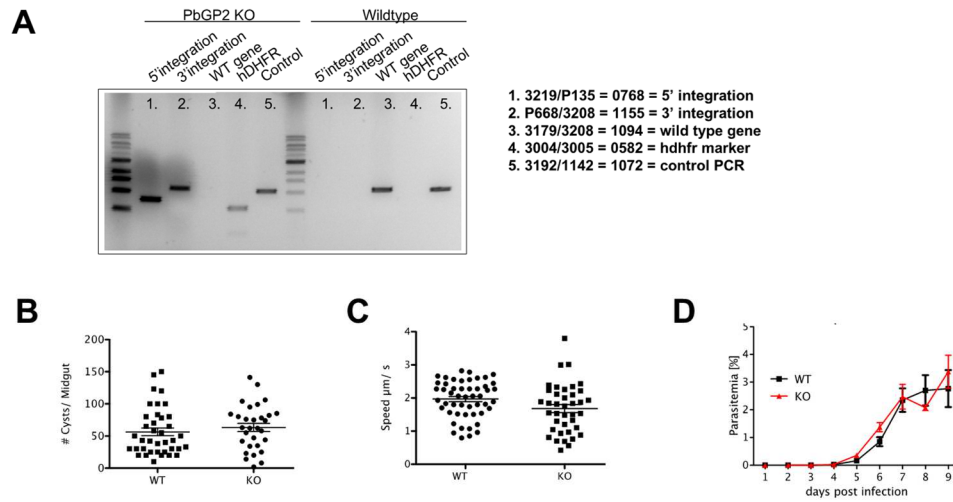


**Figure 6: PbGP2 is not essential for the mosquito stages and for virulence in mice.** (A) PCR genotyping of a *P. berghei*  $\Delta$ gp2 gene deletion mutant corroborating the integration of knock out plasmid pLIS0385 into the PBANKA\_0924800 locus. (B) Oocyst infection numbers of  $\Delta$ gp2 (n=38) compared with the wild type reference line (n=30). (C) Gliding motility speed of  $\Delta$ gp2 (n=50) and wild type parasites (n=39). (D) Infection dynamics determined by injection of 10k  $\Delta$ gp2 or wild type salivary gland sporozoites shows no difference in virulence.

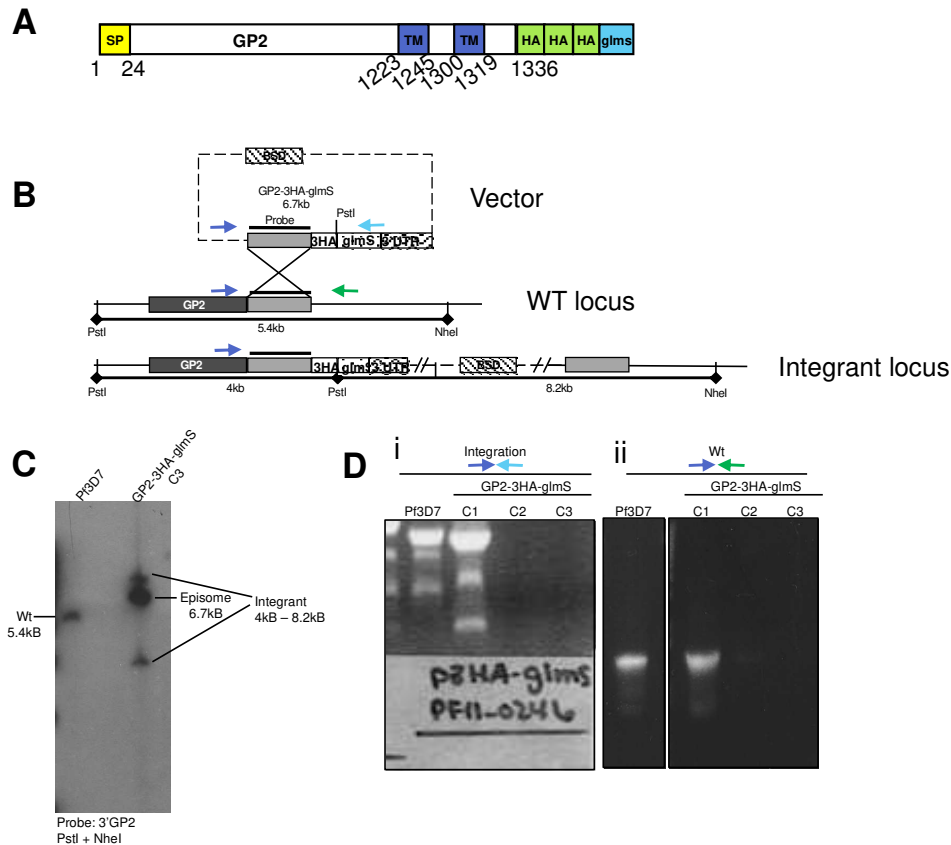


**Figure S1: Generation of the GP2-3HA-glmS tagged line.** (A) Schematic representation of the GP2 protein with two transmembrane domains (TM) and a signal peptide (SP). The tagged line is represented with the triple hemagglutinin (HA) and the glucosamine-inductible glmS ribozyme (glmS). Amino acid numbers are indicated underneath. (B) Schematic of the knock-in strategy to integrate the 3HA-glmS cassette in 3'UTR of the *GP2* gene by single crossover homologous recombination. Arrows correspond to the position and orientation of the primers used for PCR tests. Restriction sites used for the Southern blot experiment and the resulting size of the digested fragments are also indicated. Probe used is indicated by a bold line. (C) Southern blot showing the integration of the 3HA-glmS cassette and the loss of the band associated with the wildtype allele after three Blasticidin selection cycles and parasite cloning. The probe used corresponds to nucleotides 2959 to 4008 of *GP2*. (D) PCR confirming the integration of 3HA-glmS at the 3' end of the *GP2* endogenous locus (i). PCR was performed on parasites from each Blasticidin selection cycle (C1, C2 and C3). *P. falciparum* 3D7 is used as wildtype locus control (ii). Primers used are indicated above with a color code referring to the schematic in (B). Note that the whitish shadow on lanes C2 and C3 of D1 is due to leftover sticky tape.

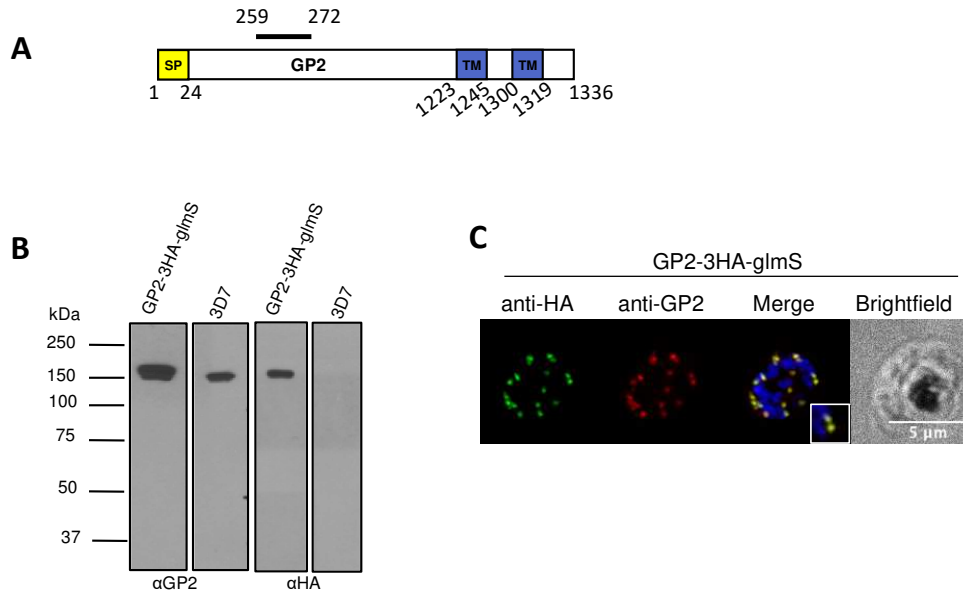
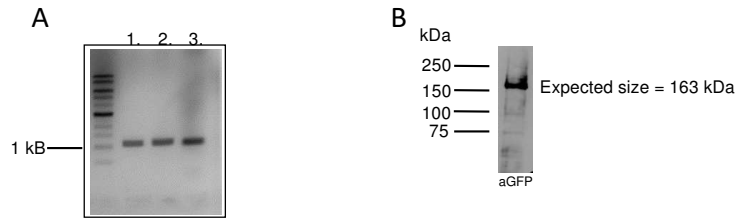


**Figure S2: Generation of a specific antibody against GP2.** (A) Schematic representation of the GP2 protein. The bar above represents the region recognized by the specific rabbit anti-GP2. Amino acid numbers are indicated underneath. (B) Western Blot shows that the anti-GP2 recognizes a single band at 150kDa in GP2-3HA-glmS and in wildtype 3D7 and the anti-HA recognized GP2-3HA in the tagged line only. (C) IFA on GP2-3HA-glmS schizont parasites shows extensive overlap between the anti-HA signal (green) and the anti-GP2 signal (red). Scale bars represent 5  $\mu$ m.



1. 3179/0408 = 1153 = 5' integration of the plasmid
2. P668/3185 = 1162 = 3' integration of the plasmid
3. 3192/1142 = 1072 = control PCR

**Figure S3: Tagging of PbGP2 with GFP.** PCR genotyping of *Pb $g$ p2::gfp* parasites corroborating the integration of plasmid pLIS0383 into the endogenous locus. (B) Western blot analysis of mixed blood stage parasites with anti-GFP revealing a GP2::GFP fusion protein of the correct expected size of 163 kDa.

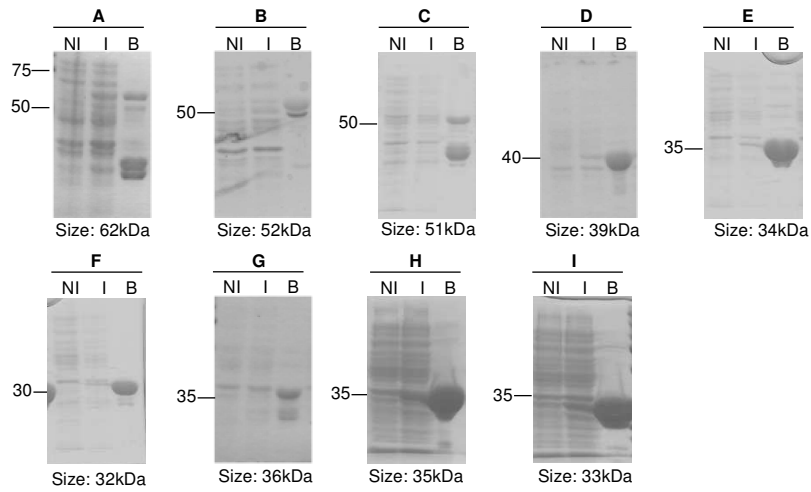


**Figure S4: GST-GP2 fragments expressed as recombinant proteins.** Coomassie-stained gels showing the induction and the purification of the recombinant GST-GP2 fragments. The expected sizes of the purified recombinant proteins are indicated below each image. For some fragments (A, B, C, G), a band at 26kDa likely corresponding to some GST degradation product is also observed. NI: non-induced; I: induced; B: purified protein.

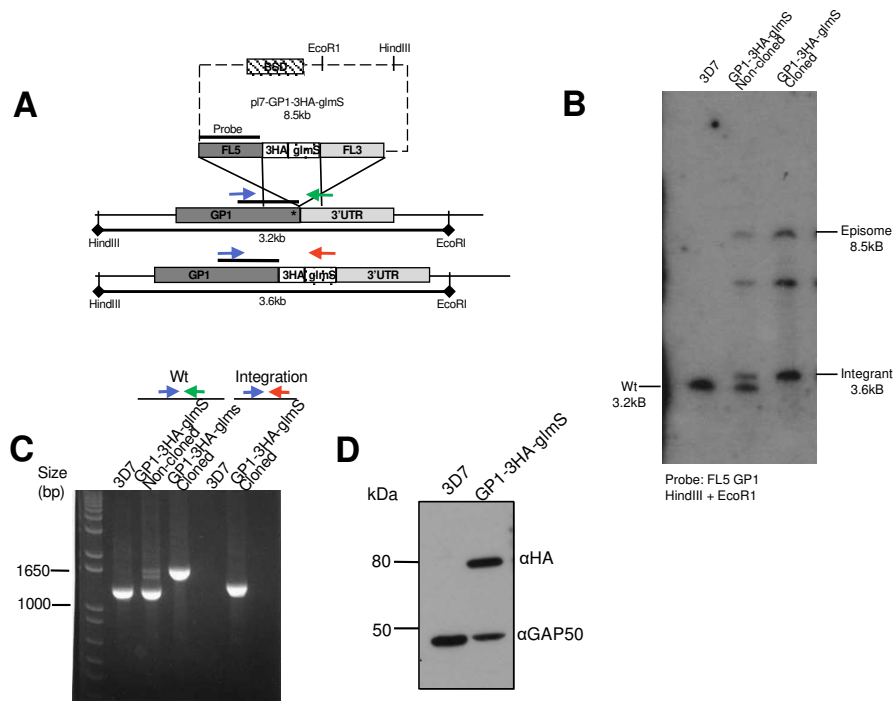


**Figure S5: Generation of the GP1-3HA-glmS tagged line.** (A) Schematic of the knock-in strategy to integrate the 3HA-glmS cassette in 3'UTR of the *GP1* gene by double crossover homologous recombination using the CRISPR Cas9 technology. Arrows correspond to the position and orientation of the primers used for PCR testing. Restriction sites used for the Southern blot experiment and the resulting sizes of the digested fragments are also indicated. Probe used is indicated by a bold line. \* represents the position of the gRNA at the 3' end of *GP1* gene. (B) Southern blot showing the integration of the 3HA-glmS cassette and the loss of the band associated with the wild type allele before and after parasite cloning. *P. falciparum* 3D7 gDNA is used as wildtype locus control. The probe used corresponds to the FL5 purified PCR fragment used for the cloning process. (C) PCR confirming the integration of 3HA-glmS at the 3' end of the *GP1* endogenous locus. PCR were performed on parasites before and after parasite cloning and on *P. falciparum* 3D7 gDNA as control. Primers used are indicated above with a color code. (D) Western blot showing the expression of GP1-3HA in the GP1-3HA-glmS tagged line but not in 3D7 (negative control). Expression was detected by Western blot using an anti-HA and an anti-GAP50 as loading control.

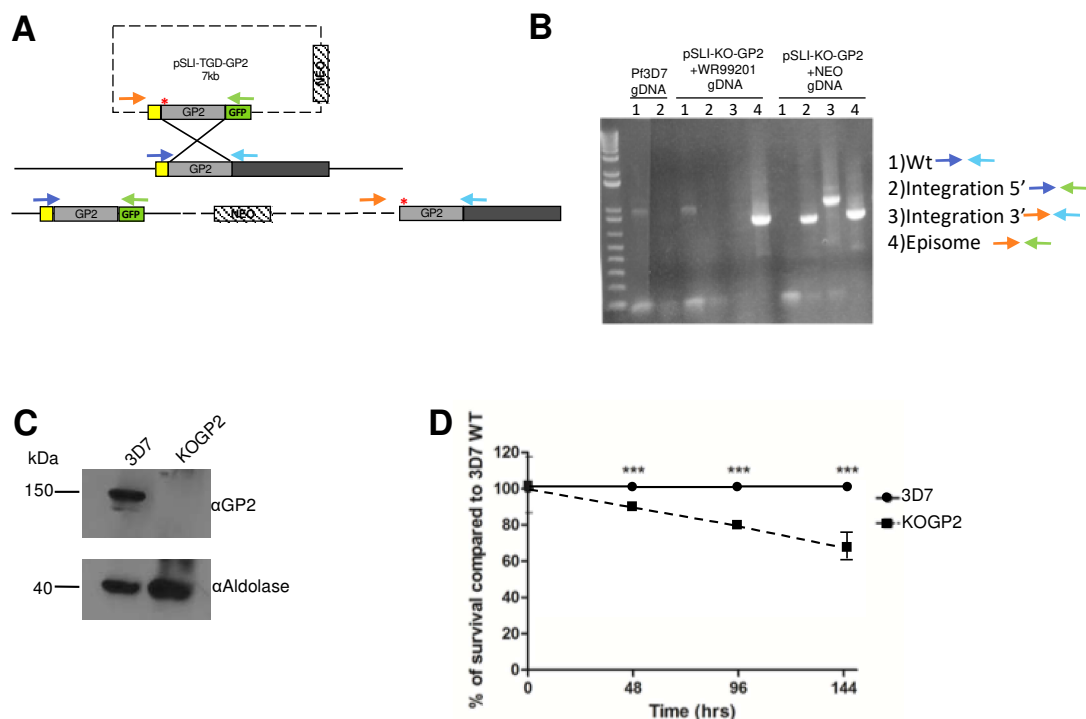


**Figure S6: Strategy to knockout *GP2* in the *GP1-3HA-glmS* line.** (A) Schematic of the selection-linked integration (SLI) strategy to knockout (KO) *GP2* in 3D7. A region at the 5' end juxtaposed to the signal peptide is used as homologous region for the integration of the *GFP* and the selection marker by single crossover homologous recombination (light grey). Primers used to test the KO by PCR are indicated by colored arrows. Neo: neomycin phosphotransferase resistance gene; \*: stop codon. (B) PCR analysis showing the integration of *GFP-NEO* at the *GP2* locus with no wildtype allele remaining after neomycin selection. (C) Western blot using the anti-*GP2* antibody to show the absence of *GP2* in the KOGP2 line. An anti-aldolase was used as a loading control. (D) Growth curve analysis showing that knocking out *GP2* in the 3D7 WT line results in an around 30% decrease in parasitemia over 3 cycles. N=6 biological replicates. \*\*\*=  $p < 0.001$ ; Two-way ANOVA followed by a Tukey multiple comparison test was used.

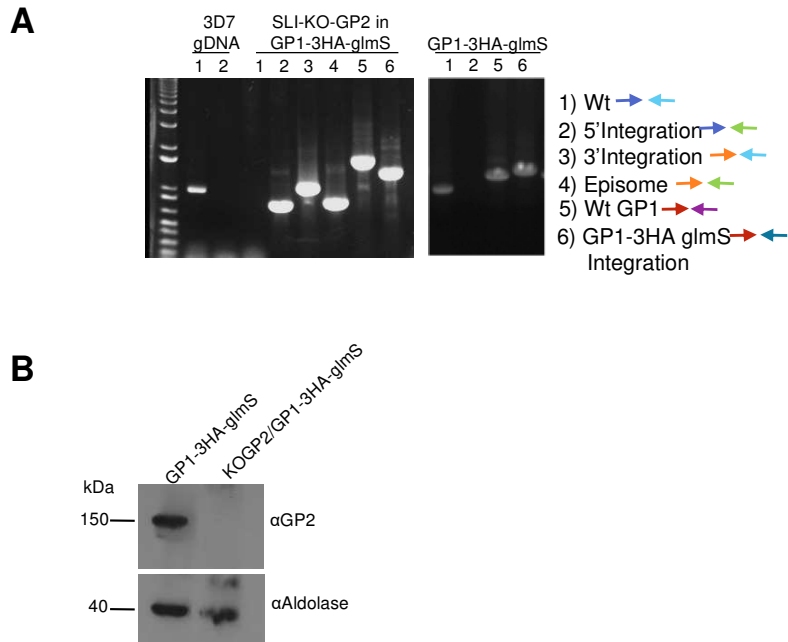


**Figure S7: Knocking out *GP2* by SLI-TGD in the *GP1-3HA-glmS* line.** (A) PCR analysis showing the integration of *GFP-NEO* at the *GP2* locus with no wildtype allele remaining after neomycin selection. We also confirmed that the 3HA-glmS at the 3' end of *GP1* gene was still present by PCR. (B) Western blot using an the anti-*GP2* antibody to show the absence of *GP2* in the *KO GP2/GP1-3HA-glmS* line. An anti-aldolase was used as a loading control.

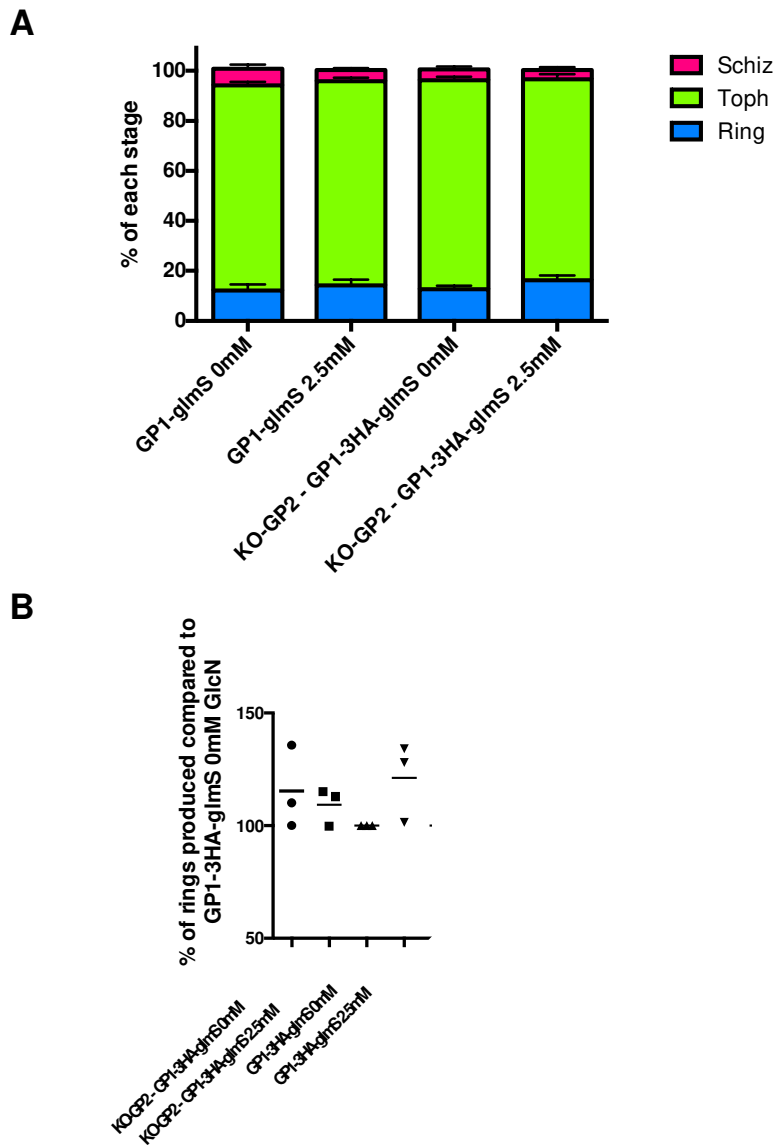


**Figure S8: GP1 knockdown/GP2 knockout parasites have a normal asexual cycle development cycle and no defect in merozoite invasion.** (A) The distribution of the different parasite stages after 3 growth cycles is the same for all conditions tested. N= 4 biological replicates. A Dunnet's multiple comparisons test was used. (B) No significant invasion defect is observed in merozoites with knocked down GP1 and knocked out GP2. N=3 biological replicates

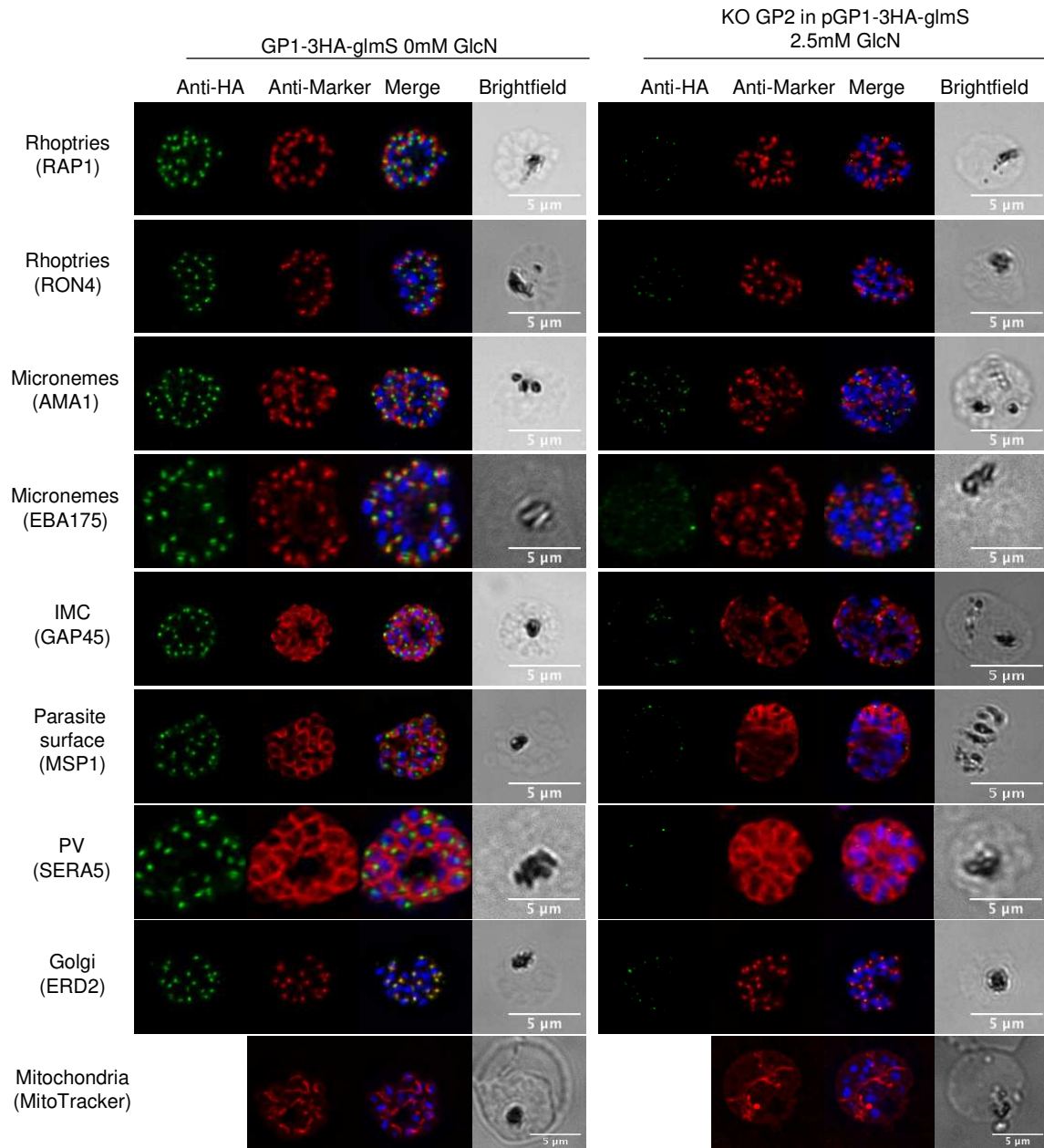


**Figure S9: The effect of the absence of GP1 and GP2 on some organelle markers observed by IFA.** Immunofluorescence assay on wildtype parasites (GP1-3HA-glmS 0mM GlcN) and on parasites lacking both proteins (KO GP2 in GP1-3HA-glmS 2.5mM GlcN). Markers for different parasite organelles were tested in combination with an anti-HA. Scale bar=5  $\mu$ m.

**Table S3. Proteins identified in both GP1 and GP2 immunoprecipitations**

	<b>Identification</b>	<b>Accession number</b>
Proteins of interest	GP1	PF3D7_1320000
	conserved <i>Plasmodium</i> protein, unknown function (GP2)	PF3D7_1123500
ERAD pathway associated	protein disulfide isomerase (PDI-11)	PF3D7_1134100
	ubiquitin-activating enzyme E1 (UBA1)	PF3D7_1225800
Mitochondria	malate:quinone oxidoreductase, putative	PF3D7_0616800
	ferrodoxin reductase-like protein	PF3D7_0720400
RNA	glutamine--tRNA ligase, putative	PF3D7_1331700
	RNA binding protein, putative	PF3D7_0605100
Others	6-phosphofructokinase (PFK9)	PF3D7_0915400
	merozoite surface protein 1 (MSP1)	PF3D7_0930300
	exportin 1, putative	PF3D7_0302900

**Table S4: List of primers used in this study.**

Sequence	Description	Use
<i>Plasmodium falciparum</i>		
5'- CCGCGGCCGCGGTGAGGGAGAAATGTTACAGG -3'	NotI-GP2-2959-fw	Cloning GP2-3HA-glmS
5'- GCC CTA GGT CTATGT AAT TTATGT TGT CTG -3'	AvrII-GP2-stopless-rev	
5-CGGGATCCGCAAAGGCAGCAAACCCAATGGAGC-3'	BamHI-GP2-A-fw	Cloning GP2 fragments in pGEX-6P3
5'-GCCTCGAGTCTTTTTCTTCATTATTCATTCAACATC-3'	XhoI-GP2-A-rev	
5'-CCGGATCCAAGAAAAGTAAATGTTTGAAG-3'	BamHI-GP2-B-fw	
5'-CCCTCGAGCAAAAAAGAAATAATAATTATAATAATTT-3'	XhoI-GP2-B-rev	
5'-CCGGATCCAGTAGTAATAATAATAGTAGTAG-3'	BamHI-GP2-C-fw	
5'-GGCTCGAGTAACATAGATTGAAAGATCTCCCATG-3'	XhoI-GP2-C-rev	
5'-CCGGATCCAACAATTTATTGAATAGTGAAAAAT-3'	BamHI-GP2-D-fw	
5'-GGCTCGAGTCCATATTATCATTCTGTACATTCAC-3'	XhoI-GP2-D-rev	
5'-CCGGATCCAACAATTTATTGAATAGTGAAAAAT-3'	BamHI-GP2-E-fw	
5'-CCCTCGAGTTTTCTTTTAAACATGGAAAAAT-3'	XhoI-GP2-E-rev	
5'-CCGGATCTATAATCCATATTCTTATGAAAG-3'	BamHI-GP2-F-fw	
5'-CCCTCGAGTCTTTTTCTTCATTATTCATTTC-3'	XhoI-GP2-F-rev	
5'-CCGGATCCAACAATTTATTGAATAGTGAAAAAT-3'	BamHI-GP2-G-fw	
5'-GGCTCGAGTATTATATCATTCAAAATTTTTCTTTC-3'	XhoI-GP2-G-rev	
5'-CGGGATCCAATAAAAGTGAACAAGAAATATTAAG-3'	BamHI-GP2-H-fw	
5'-GGCTCGAGTCCATATTATCATTCTGTACATTCAC-3'	XhoI-GP2-H-rev	
5'-CGGGATCCAATAAAGAATGTGAGTGAGAATAATG-3'	BamHI-GP2-I-fw	
5'-GGCTCGAGTCCATATTATCATTCTGTACATTCAC-3'	XhoI-GP2-I-rev	
5'-GGCTCGAGGATATACTTCTATTTTAGAACAAAG-3'	XhoI-GP1-FL5-fw	Cloning FL5 for CRISPR strategy
5'-ACCCCGGGTGTTTTATTTGGAAACTTCATATATTGTACTAACATGTGACCGATAAAATTCATGTGAATA-3'	XmaI-GP1-FL5-stopless-G3744A-T3732C-rev	
5'-GCCC CGG AAAAAAAAAAGAAAAAGAAAAAGAAAAAATAAG-3'	SacII-GP1-FL3-fw	Cloning FL3 for CRISPR strategy
5'-CGACTAGTCTGCAACAAAACGGATTAACCGTTTCTATTATCCACGAG-3'	SpeI-GP1-FL3-rev	
5'-TAAGTATATAATATTTGAATT TATGGTCACATGTTGGGTTTAGAGCTAGAA-3'	BtgZI-GP1-gRNA-fw	Cloning gRNA for CRISPR strategy
5'-TTCTAGCTCTAAAACCAACATGTGACCAATAAATTCAAATATTATATACTTA-3'	BtgZI-GP1-gRNA-rev	
5'-AGGCGGCCGCTAAGTATATTATTTAATTGGTGTTCAC-3'	NotI-GP1-fw	Cloning KO-GP1
5'-GCACGCGTGAATGTTTAATAAATCTTCAGAAAC-3'	MluI-GP1-497-rev	
5'-ACGCGGCCGCTAAACATGTTTCATCCAATAATAATAATAG-3'	NotI-GP2-55-fw	Cloning KO-GP2
5'-CGACGCGTCAAATCTCCAAATATTTGCACATAATTATC-3'	MluI-GP2-540-rev	

Sequence	Description	Use
<i>Plasmodium falciparum</i>		
5'- GAGGATGATGTATTATTAAGTGGT -3'	Upstream-GP2-fw	Genotyping integration at GP2 locus
5'-GTGATCTGGAGAAGAAAACATTTTATAAGCC-3'	Downstream-GP2-rev	Genotyping integration at GP2 locus
5'- GCATGCAAGCTTATAATTATTAATAGG -3'	3HA-glmS vector-fw	Genotyping glmS integration
5'-GGTACCAGATCATGTGATTTCTCTTTG-3'	glmS-rev	Genotyping glmS integration
5'-CGATTTTACCAGTATCAGCAACA-3'	Upstream-GP1-fw	Genotyping integration at GP1 locus
5'-GCTATGATAACGCCATTTTTATTTAAACAAAAGGTTGTA-3'	Downstream-GP1-rev	Genotyping integration at GP1 locus
5'-CGCCTAGGATGAATATTTTTAAAAGATATATAT-3'	GP2-fw	Genotyping GFP integration KO strain
5'-CGCTTAAGTCACCATCATTATGTCCTTGATCAAATATC-3'	GP2-992-rev	Genotyping GFP integration KO strain
5'-AGGTAGTTT TCCAGTAGT GC-3'	GPF-rev	Genotyping GFP integration KO strain
5'-GGAATTGTGAGCGGATAACAATTTACACAGG-3'	pSLI-vector-fw	Genotyping GFP integration KO strain
<i>Plasmodium berghei</i>		
5'-TAAAAGGGTACAAAAATG -3'	g3179	pLIS0383 GP2 GFP tag
5'-AAAGGATCCTAGGTGTAATTTTCTCTT-3'	g3180	pLIS0383 GP2 GFP tag
5'-TAAAAGGGTACAAAAATG -3'	g3179	gp2 ::gfp genotyping
5'-GTATGTTGCATCACCTTC-3'	g0408	gp2 ::gfp genotyping
5'-TGATTAGCATAGTTAAATAAAAAAAGTTG-3'	P668	gp2 ::gfp genotyping
5'-TAAAACGTTTGTATATGC-3'	g3185	gp2 ::gfp genotyping
5'-GTACAAGATTTAAATCAACC-3'	g3192	gp2 ::gfp genotyping
5'-CTGCAAATTTATATTAGC-3'	g1142	gp2 ::gfp genotyping
5'-AAAGGTACCACATTATACGTACATGC-3'	g3177	pLIS0385 Δgp2
5'-ATTATAACAATATGATAG-3'	g3178	pLIS0385 Δgp2
5'-TAAAAGGGTACAAAAATG -3'	g3179	Δgp2 genotyping
5'-AAAGGATCCTAGGTGTAATTTTCTCTT-3'	g3180	Δgp2 genotyping
5'-GTTTCATGTTCAAATTGGC-3'	g3219	Δgp2 genotyping
5'-GTAAACTTAAGCATAAAGAGCTCG-3'	P135	Δgp2 genotyping
5'-TGATTAGCATAGTTAAATAAAAAAAGTTG-3'	P668	Δgp2 genotyping
5'-TATTTTCTGAGTTCGAC-3'	g3208	Δgp2 genotyping
5'-AAAAGATCTATGGTTGGTTCGCTAAACTG-3'	g3004	Δgp2 genotyping
5'-AAACAATTGTTAATCATTCTTCTCATATAC-3'	g3005	Δgp2 genotyping
5'-GTACAAGATTTAAATCAACC-3'	g3192	Δgp2 genotyping
5'-CTGCAAATTTATATTAGC-3'	g1142	Δgp2 genotyping